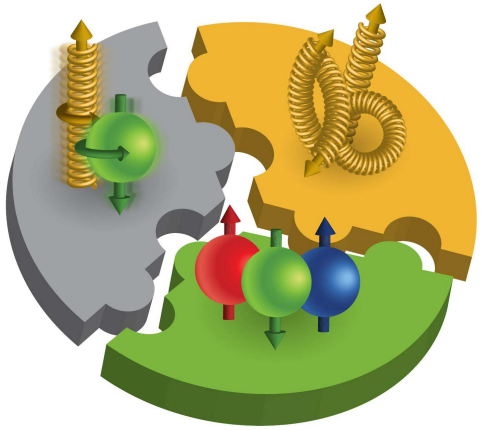

Absolute hadron beam polarimetry at EIC

Frank Rathmann

EIC Accelerator Design Weekly Meeting ☞
September 11, 2024

Initial observation

- In recent years, many groups specializing in **polarization instrumentation & technology** for hadronic probes have disappeared, along with the valuable expertise they once contributed. This contrasts sharply with the time when RHIC was conceived, when numerous experimental and theoretical groups from around the world provided a wealth of expertise.
- Currently, we face a critical situation, with a shortage of skilled individuals, which is crucial to overcome for the EIC's success.
- There is an urgent need to rejuvenate polarization instrumentation & technology for hadrons and expand education and training efforts.[1].

[1] Key areas are highlighted in https://technotes.bnl.gov/PDF?publicationId=225693

Contents I

Hadron polarimetry requirements for the EIC I

Comments

- The EIC will use polarized **protons** and **helions**, later on possibly deuterons, and heavier nuclei like lithium may be needed.
- **The EIC promises to provide proton beam polarizations over 70% with a relative uncertainty of 1% or less.**
- Polarization calibration needed for each ion species as is presently done. Via $\vec{p}\vec{p}$ elastic scattering (identical particles) $\Rightarrow$ beam polarization inferred from known target polarization.
- **Absolute proton beam polarization calibration relies on precisely measured nuclear polarization of atomic jet using Breit-Rabi polarimeter.**

Hadron polarimetry requirements for the EIC II

Polarimeters shall determine:

- Bunch polarization profile in x, y, and z
- Polarization lifetime
  - For EIC physics, projection of $\vec{P}$ on stable spin axis required, no in-plane polarization.
- Polarization vector $\vec{P}$ per bunch

Instruments

- Hadron polarimeter (absolute) in IP4
- pC polarimeter (relative) in IP4 and IP6 (between spin rotators)

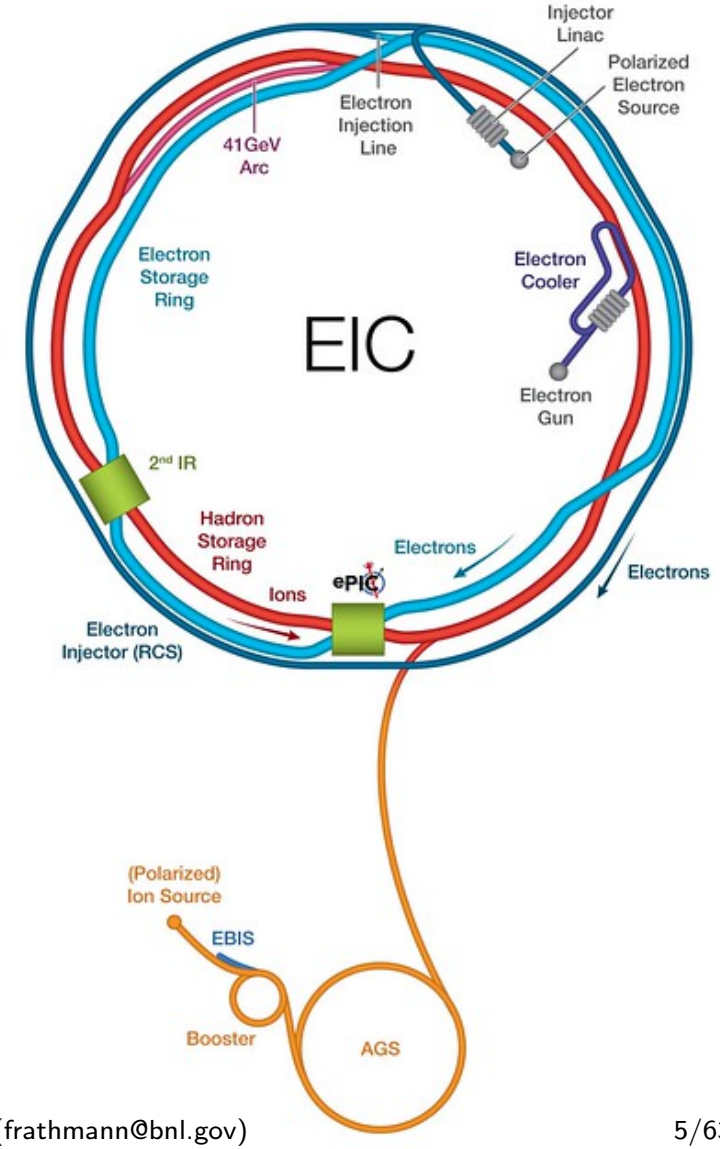

Asymmetry and polarization

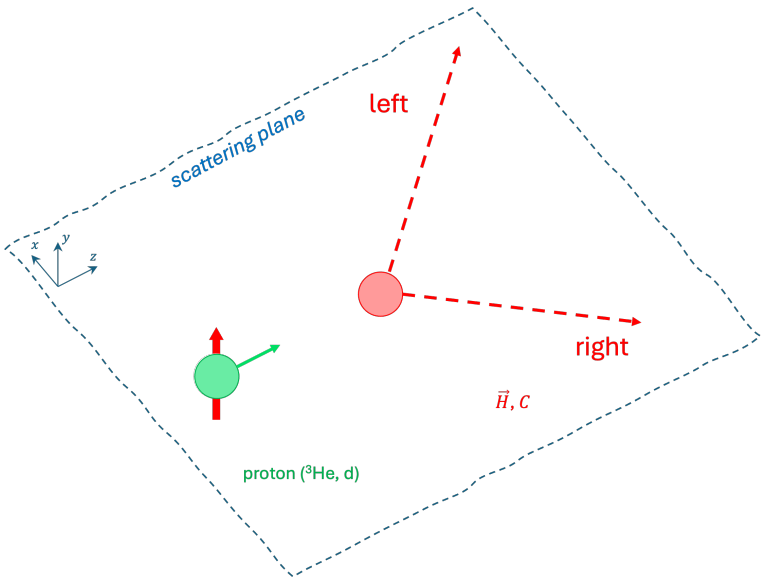

- Spin-dependent cross section

$$\sigma = \sigma_0(1 + A_y P_y \cos\phi) \tag{1}$$

  - Unpolarized cross section σ_0
  - P_y vertical component of beam polarization $\vec{P} = (P_x, P_y, P_z)$
  - Analyzing power $A_y = \frac{\sigma^{\text{left}} - \sigma^{\text{right}}}{\sigma^{\text{left}} + \sigma^{\text{right}}}$
  - Azimuth of scattered particle ϕ

Coulomb-nuclear interference (CNI)

- A_y: measure of polarization sensitivity of scattering process
- **At AGS and RHIC energies, no scattering processes available with A_y known to sufficient accuracy for $\Delta P \leq 0.01$ [1].**
- **Interference of EM and strong interaction at small scattering angles provides sizable analyzing power for elastic pp (and pN) scattering.**

Coulomb-Nuclear interference I

Need for calibration

- Asymmetry from CNI region constitutes basis of RHIC high-energy (absolute) polarimeters
  - derived from same EM amplitude that generates anomalous magnetic moment

$$\mu_p = g_p \frac{e\hbar}{2m_p} = g_p \mu_N, \quad g_p \approx 5.585$$
$$g_p - 2 \approx 3.585 \Rightarrow \mu_p^{\text{anomalous}} \approx 1.792\,\mu_N \tag{2}$$

  - E704 at Fermilab used 200 GeV/c $\vec{p}$ from hyperon decay to detect asymmetry in scattering from H target [2]. Largest $A_y \approx 0.04$ with large statistical errors.
  - Meanwhile, accurate measurements of A_y are available from RHIC [3]
- Asymmetry measurements involve normalization uncertainties and calculations of A_y are subject to uncertainties in amplitudes of strong interaction. **Therefore, accurate calibration of reaction required.**

Coulomb-Nuclear interference II

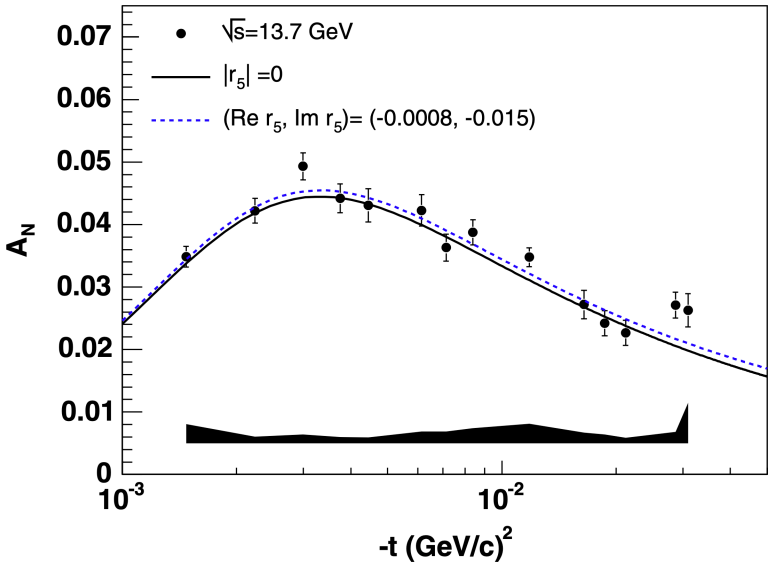

Measured A_N from RHIC in the CNI region at $\sqrt{s} = 6.8\,\text{GeV}$ ($E_{\text{lab}} = 23.7\,\text{GeV}$) [3].

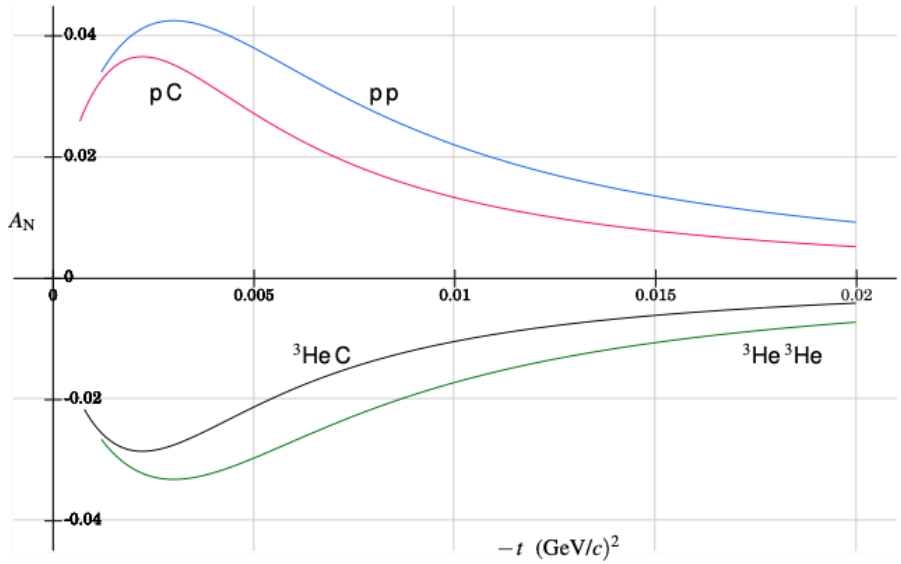

Calculation of A_y in the CNI region by Nigel Buttimore [4].

Instruments for absolute and relative polarimetry

Two devices

- **HJET polarimeter**

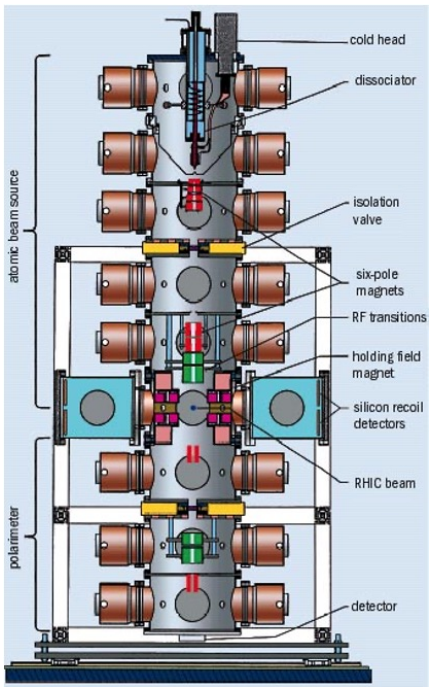

  - **absolute, slow**

$$\frac{\Delta P}{P} \approx 3\% \text{ per } 4 \text{ hour} \qquad (3)$$

- **pC polarimeters**

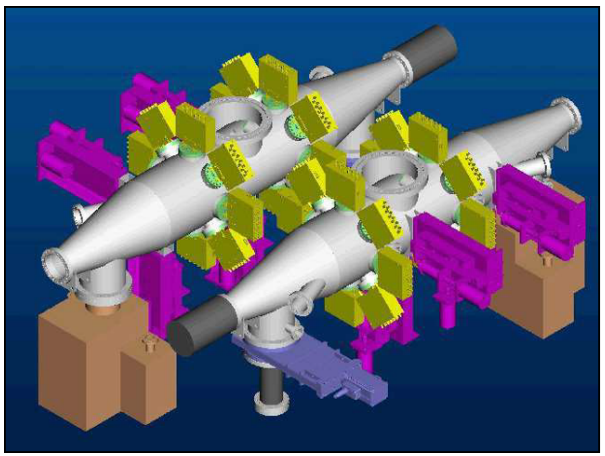

  - **fast, relative**
  - transverse profiles of polarization

$$\frac{\Delta P}{P} < 1\% \text{ per scan} \qquad (4)$$

Detector system at the polarized jet target

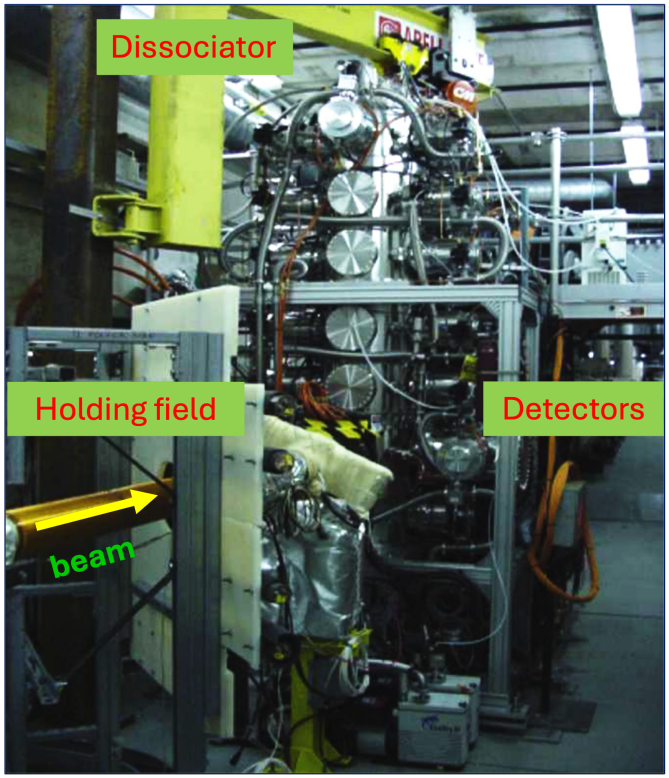

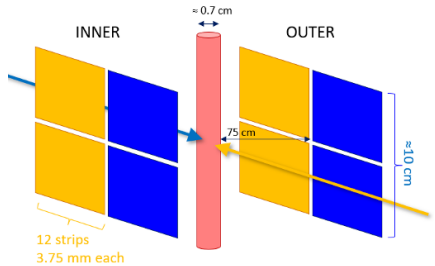

Eight Si strip detect.

- 12 vertical strips
- 3.75 mm pitch
- 500 µm thickness

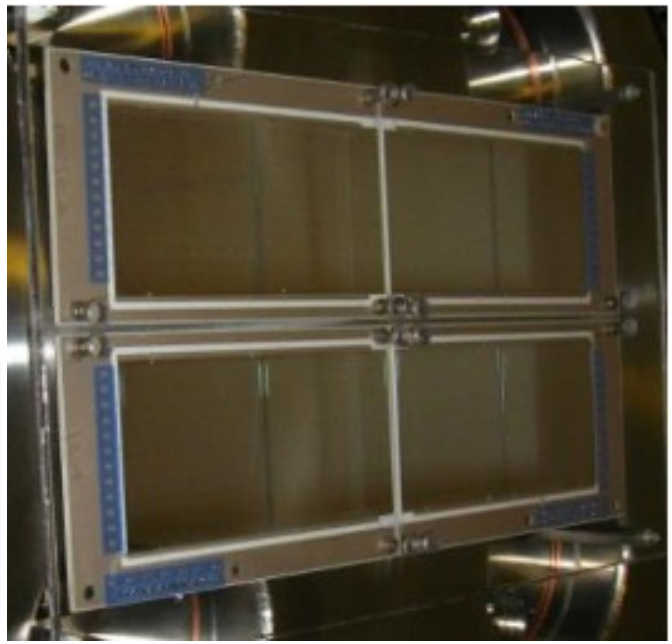

With present setup of L-R detectors and guide field B_y

- Only vertical component P_y measurable via L-R asymmetry near $\theta = 90°$.

CNI polarimeter setup

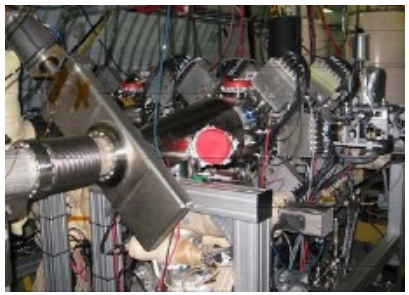

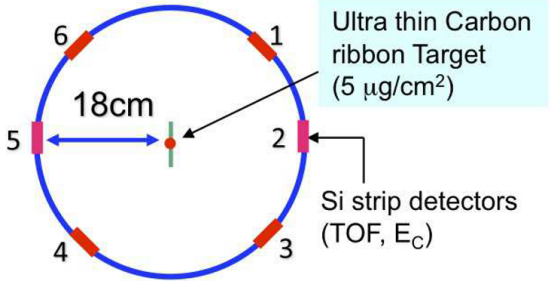

CNI setup with 6 Si detectors at different azimuth at each target enables

- determination of polarization components P_x and P_y
- determination of polarization profile along x and y
- Due to parity violation, $A_z \approx 0$ (no longitudinal analyzing power) $\rightarrow$ P_z not measurable with *unpolarized* target

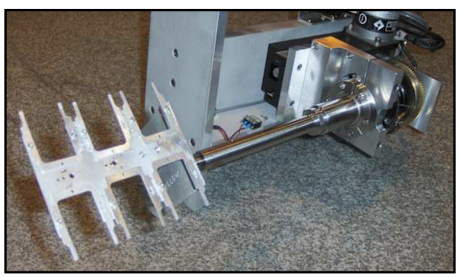

Ultra-thin ribbon targets

- 8 target holder inside beam pipe
- 2 holders per beam for x and y
- 6 targets per holders, 48 in total
- Targets $\approx 10\,\mu\text{m} \times 100\,\text{nm}$, hand crafted by D. Steski & team

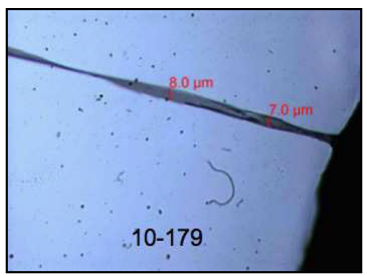

Absolute polarization from polarized hydrogen jet I

Breit-Rabi polarimeter

- Capable to determine absolute polarization Q of atomic beam, i.e., electron and proton polarization of hydrogen atoms, with accuracy $\Delta Q/Q \lesssim 1\%$.
  - Take this as a given. Will revisit subject through measurements after run 24.
  - No solid estimates available that fully encapsulate the BRP measurement systematics at the HJET on the $\approx 1\%$ level.

Beam polarization calibration

1. Proton beam passes through target of polarized H atoms of known polarization Q

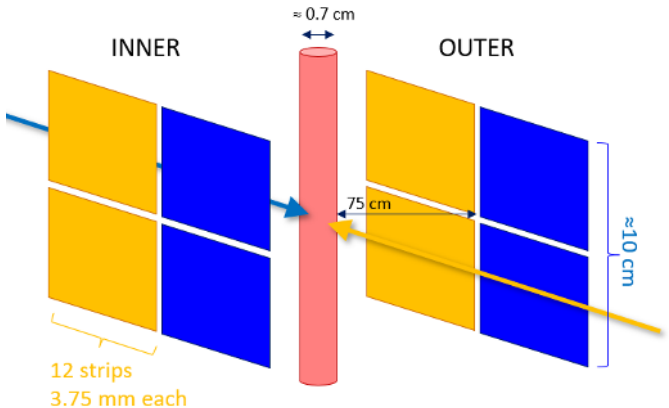

Absolute polarization from polarized hydrogen jet II

Beam polarization calibration

2. Measure number of scattered particles in left (L) and right (R) detectors
3. Sign of Q periodically reversed to compensate for asymmetries caused by differences in detector geometry or efficiency in L and R directions.
4. This determines target asymmetry

$$\epsilon_{\text{target}} = \frac{\text{L} - \text{R}}{\text{L} + \text{R}} = A_y \cdot Q \cos\phi \,. \tag{5}$$

5. Measurement of corresponding asymmetry with beam particles determines ϵ_{beam}. In elastic pp scattering, and more general in the elastic scattering of *identical* particles, A_y same regardless of which proton is polarized.
6. Absolute beam polarization given by

$$\boxed{P = \frac{\epsilon_{\text{beam}}}{\epsilon_{\text{target}}} \cdot Q} \tag{6}$$

Beam-induced target depolarization at RHIC and EIC

Polarized hydrogen jet

- Development of HJET for RHIC finished 20 yrs ago.
- Many details on the technical structure and development cannot be found in the literature. There is no comprehensive publication available.
- Grigori Atoian knows all that is needed to reliably operate the source
- Anatoli Zelenski is an excellent source of information
  - Tom Wise gave me some unfinished paper drafts and notes.
  - I am in touch with Alexander Nass about BRP operation and his most recent full polarization measurement with BRP (from 2004).
- At EIC, bunch repetition frequency much larger than at RHIC $\rightarrow$ investigate **beam-induced depolarization of target atoms** and understand situation

Bunch structure

RHIC situation:

- Time period between two adjacent bunches: $\tau_\mathrm{b} = \frac{\tau_\mathrm{rev}}{N_b} = 106.57\,\mathrm{ns}$
- Number of stored bunches $N_b = 120$
- Bunch frequency $f_\mathrm{b} = \frac{1}{\tau_\mathrm{b}} = 9.3831\,\mathrm{MHz}$
- Large number of harmonics contribute to induced magnetic high-frequency field close to RHIC beam, as bunches are short ($\sigma_t \approx 1.8\,\mathrm{ns}$)

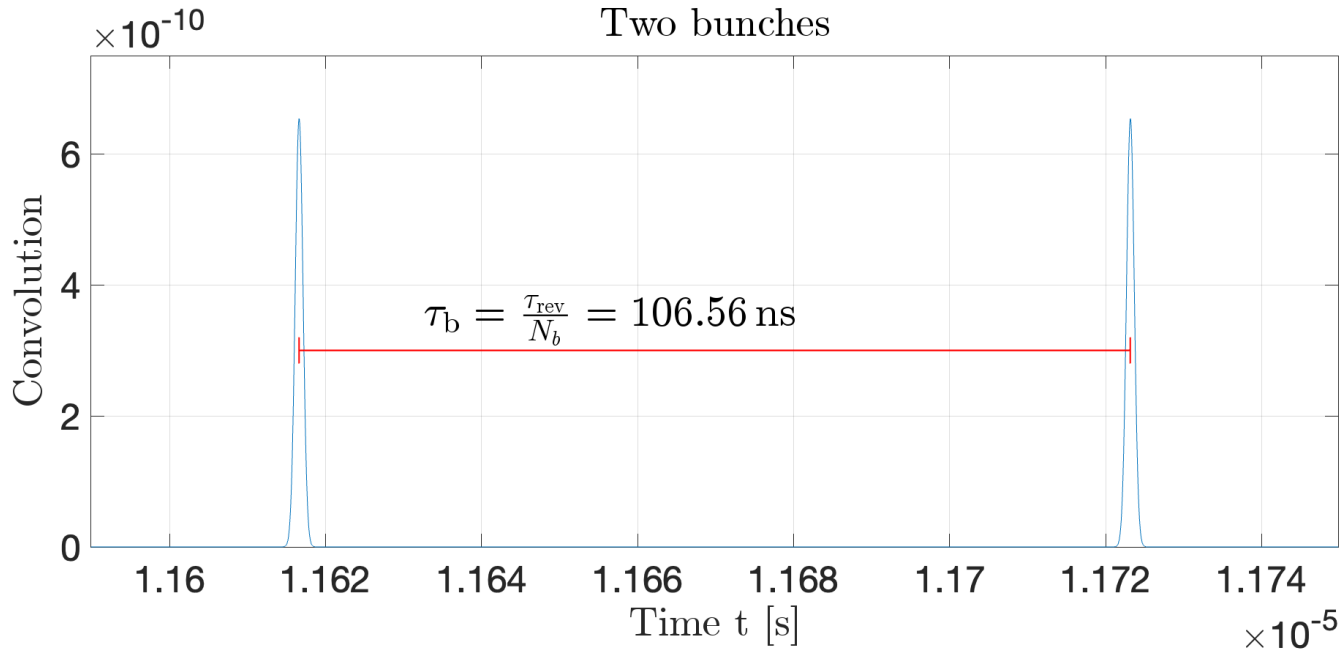

Hyperfine states of hydrogen

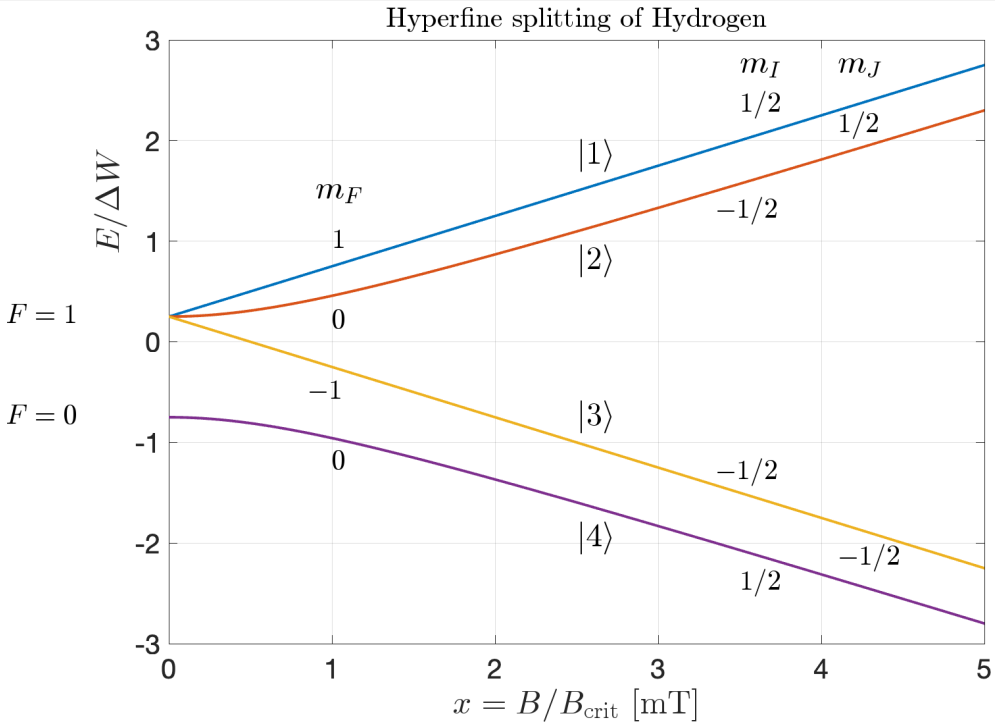

Critical field B_c (see slide 69)

- Zeeman energy $g_J \mu_B B$ comparable to E_{hfs}
- $E_{\mathrm{hfs}} \approx 5.874 \times 10^{-6}$ eV ($\approx$1420 MHz [5]):
- $B_c = 50.7$ mT

Transition frequencies

- Transition frequency between two hyperfine states $|i\rangle$ and $|j\rangle$ given by:

$$f_{ij} = \frac{E_{|i\rangle}(B) - E_{|j\rangle}(B)}{h} \tag{7}$$

- **When f_{ij} matches one of the beam harmonics at a certain holding field $|\vec{B}|$, resonant depolarization occurs [6]**

Single bunch distribution

- (Gaussian) bunch in RHIC

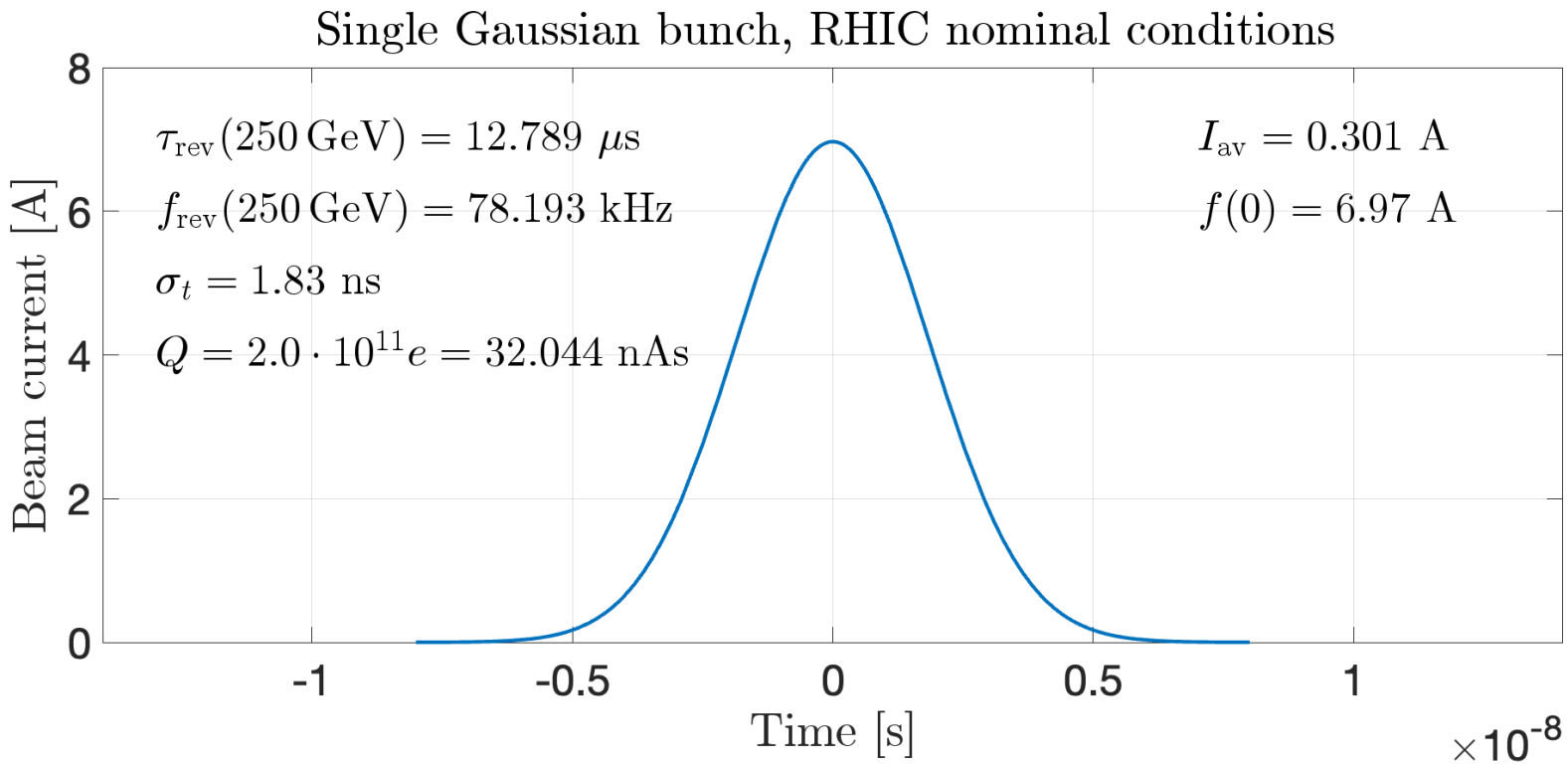

Pulse shape described by

$$f(t) = \frac{Q}{\sqrt{2\,\pi}\sigma_t} \exp\left(-\frac{t^2}{2\sigma_t^2}\right) \tag{8}$$

Gaussian convoluted with (finite) series of delta functions

Total beam current as function of time t given by

$$I(t) = \int_{-\infty}^{\infty} f(t-\xi) \sum_{k=-\infty}^{\infty} \delta\left(\xi - k\frac{\tau_{\mathrm{rev}}}{N_{\mathrm{b}}}\right) \mathrm{d}\xi \tag{9}$$

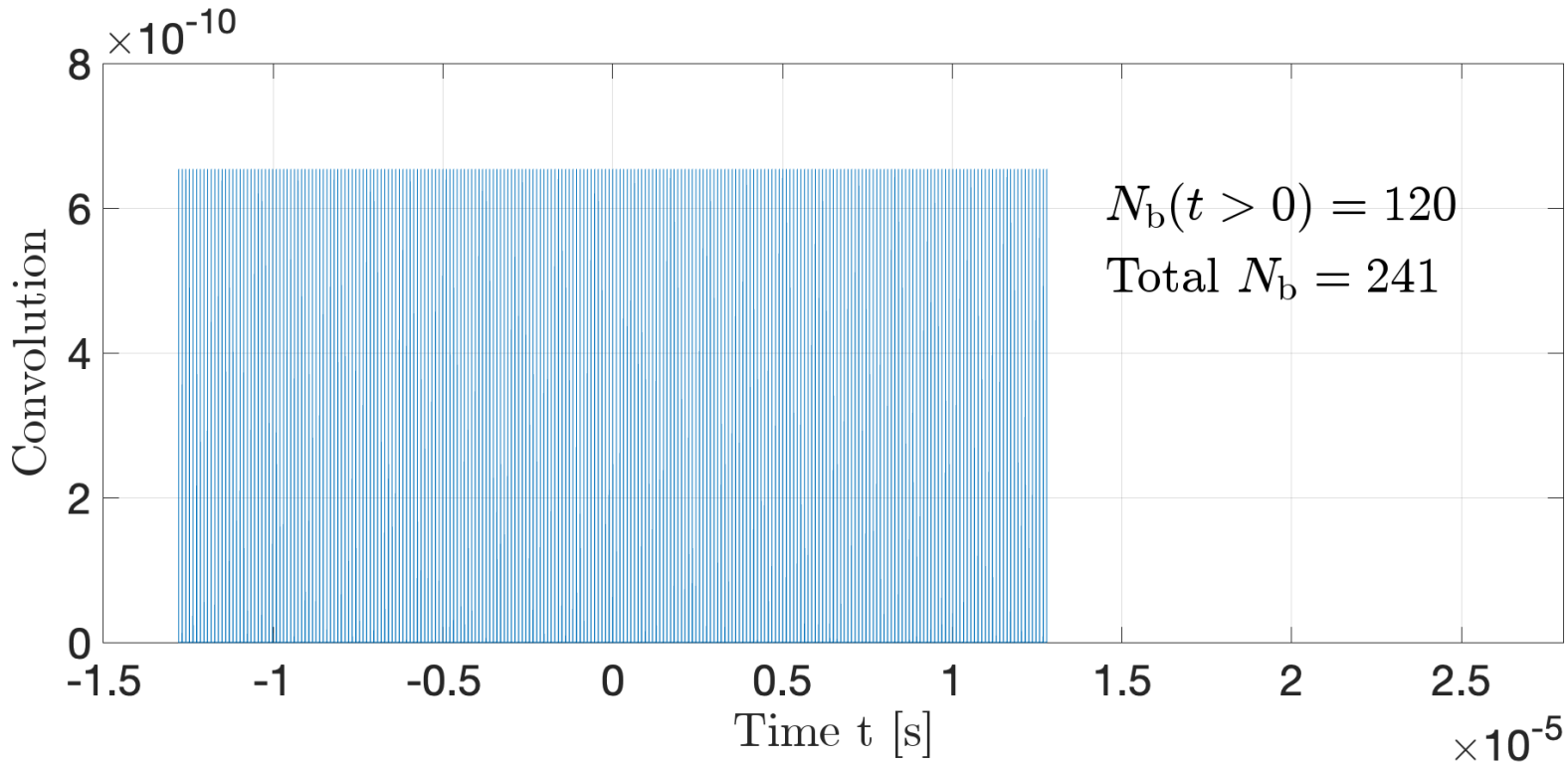

Radiofrequency-fields

FFT of convolution

- Two-sided amplitude spectrum of FFT of the convolution

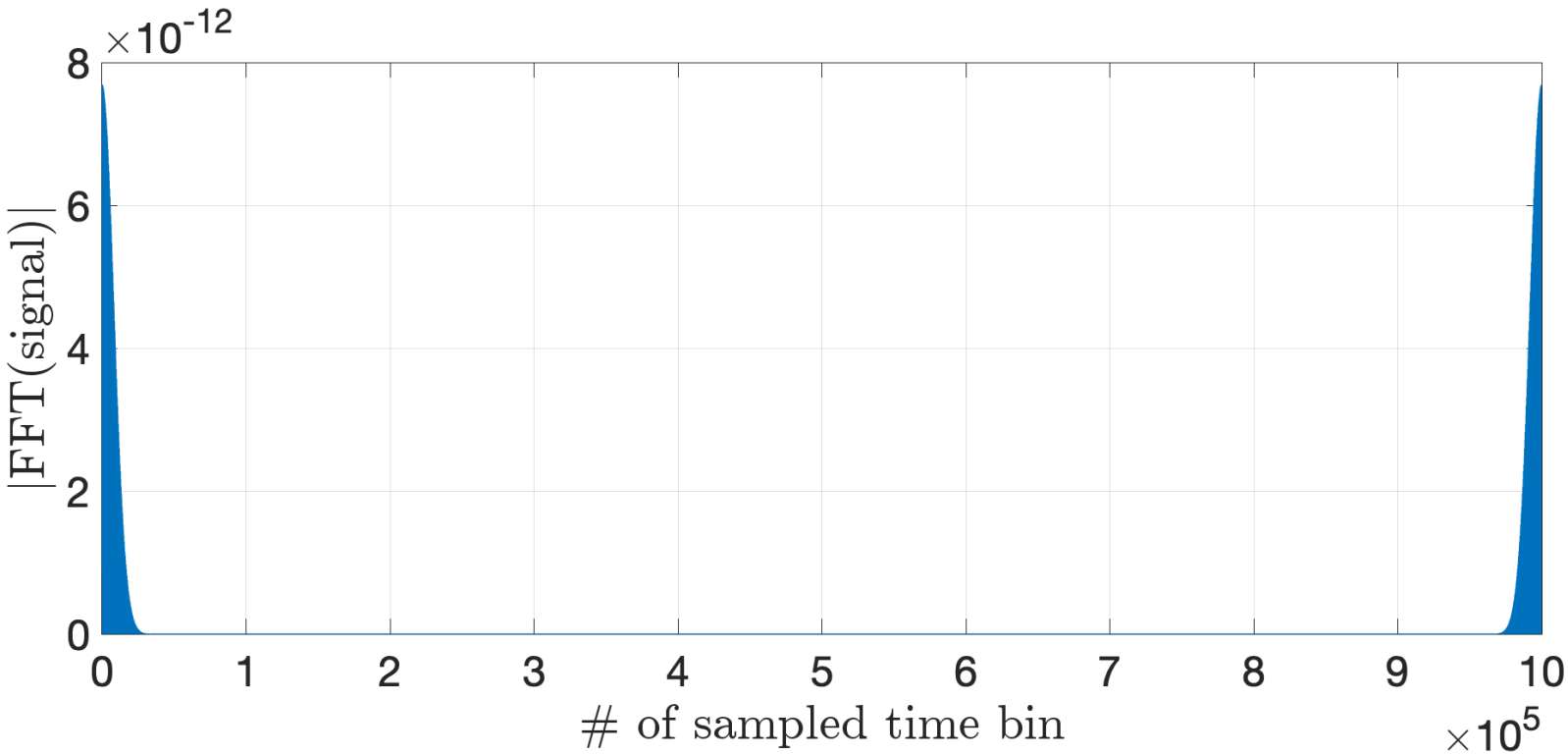

Produced radio-frequency fields

- Single-sided amplitude spectrum of FFT
- x-axis converted to frequency

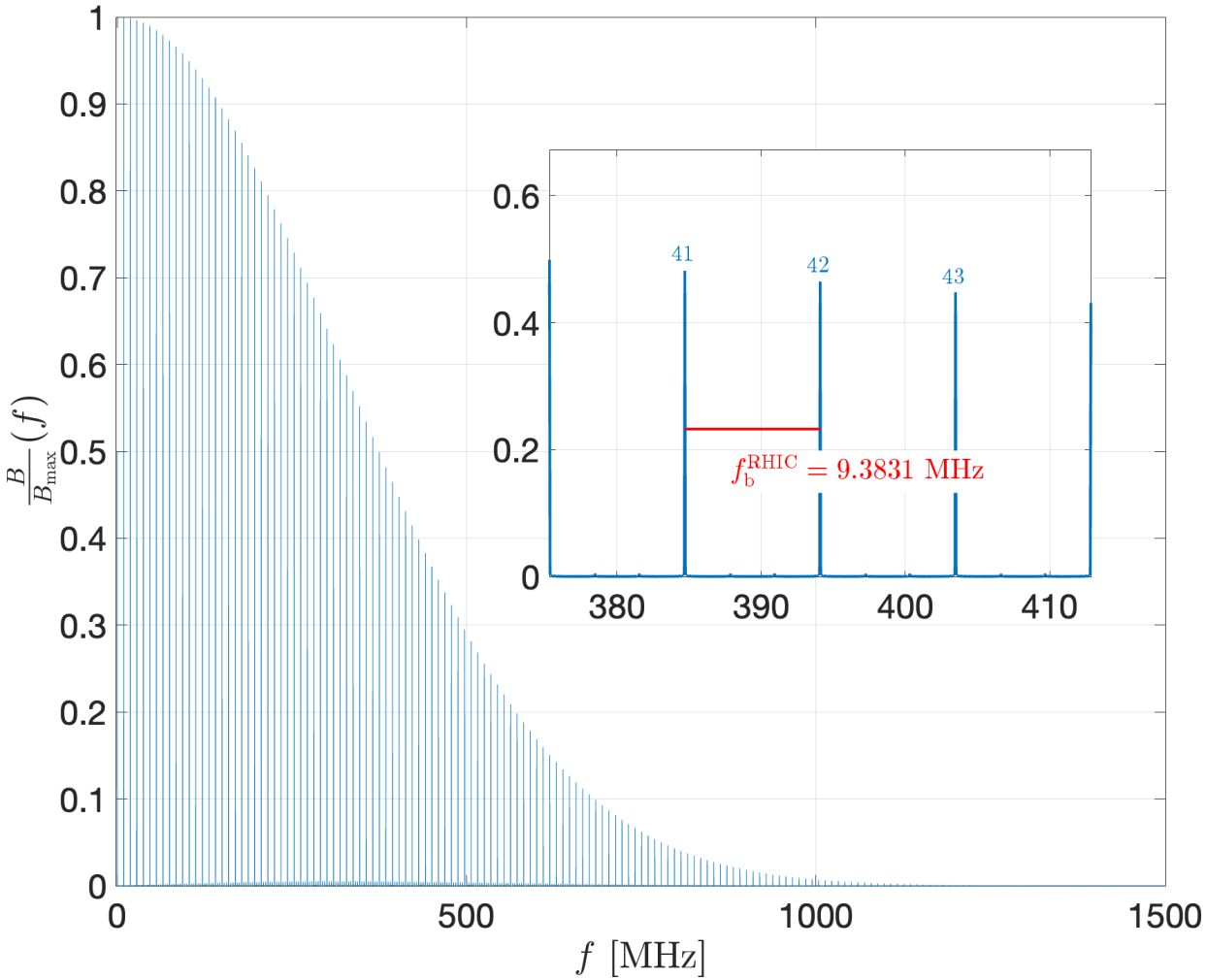

Amplitudes of magnetic RF fields

- Same, but logy
- FFT background $\leq 1\%$
  - not at f_{rev}
  - not from finite set of δ fcts
  - $\rightarrow$ probably numerical from FFT

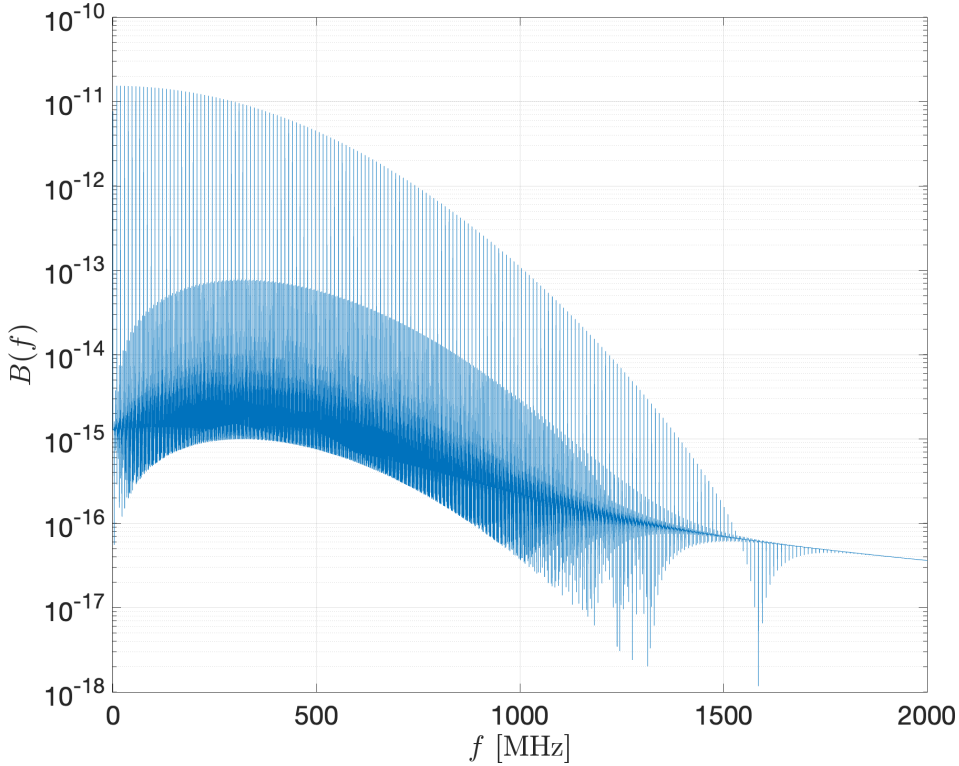

Transition frequencies between hyperfine states of H

Based on Zeeman splitting (slide 16) using Eq. (7)

- Determine transition frequencies f_{ij} between hyperfine states $|i\rangle$ and $|j\rangle$.
- Classification refers to change of quantum numbers (see Ramsey [7]):
  - B_0 is static field, B_1 is RF field that exerts torque on magnetic moment μ:
  - π ($B_1 \perp B_0$) transitions *within one* F multiplet:

$$\Delta F = 0, \quad \Delta m_F = \pm 1. \tag{10}$$

  - σ ($B_1 \parallel B_0$) transitions *between different* F multiplets:

$$\Delta F = \pm 1, \quad \Delta m_F = 0, \pm 1. \tag{11}$$

Possible transitions

- Single photon transitions in H: f_{12}^{π}, f_{23}^{π}, f_{14}^{σ}, f_{24}^{σ}, and f_{34}^{σ}.
- Transition $f_{13}^{2\gamma}$ with $\Delta m_F = 2$ requires two photons.

Transition frequencies between hyperfine states of H

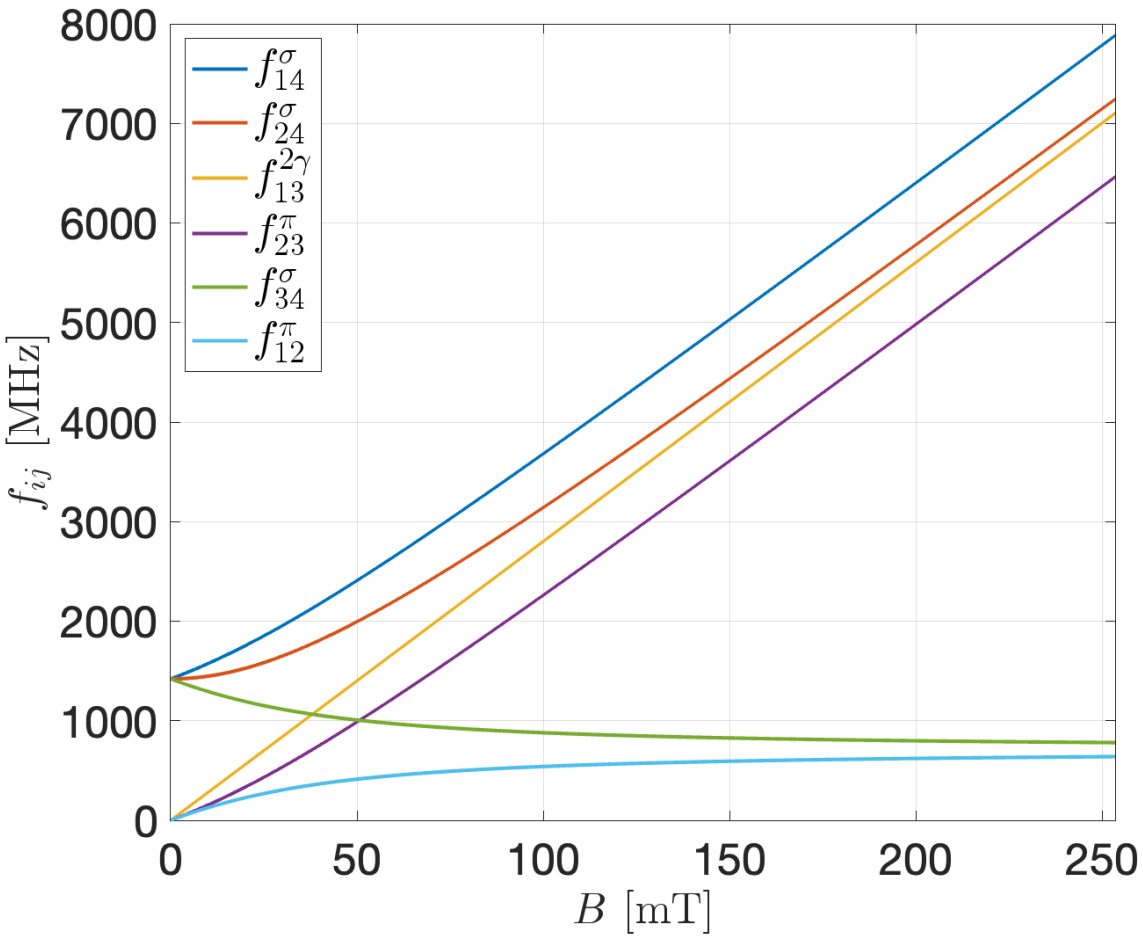

For $n = 4$ hyperfine states, $\binom{n}{2} = 6$ transitions possible.

Hyperfine transitions in H from bunch fields at RHIC

Depolarization occurs when f_{ij} multiple of bunch frequency f_b^{RHIC}

- HJET injects states $|1\rangle + |4\rangle$ ($p^{\uparrow}$) and $|2\rangle + |3\rangle$ ($p^{\downarrow}$).
  - What is exact magnitude and orientation of $\vec{B}^{\mathrm{HJET}}$?

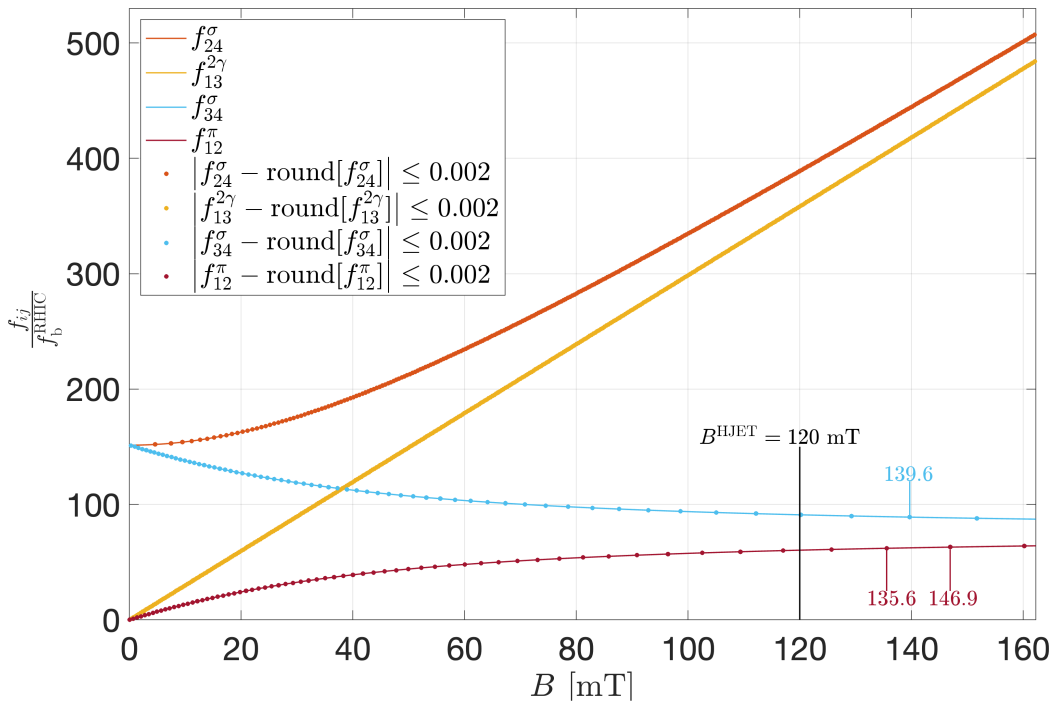

- $\left|\frac{f_{ij}}{f_b^{\mathrm{RHIC}}} - n\right| \leq 0.002\,,\ n \in \mathbb{N}$
- No depolarization from same $m_I \Rightarrow f^{\sigma}_{14},\ f^{\pi}_{23}$ omitted

HJET at RHIC operated in safe region around $B_y = 120\,\mathrm{mT}$

- At RHIC, transitions with $\frac{f_{ij}}{f_b^{\mathrm{RHIC}}} \gtrsim 350$ were ignored
- Don't know exactly at which harmonic number, depolarization sets in.

Single bunch distribution

- (Gaussian) bunch in EIC

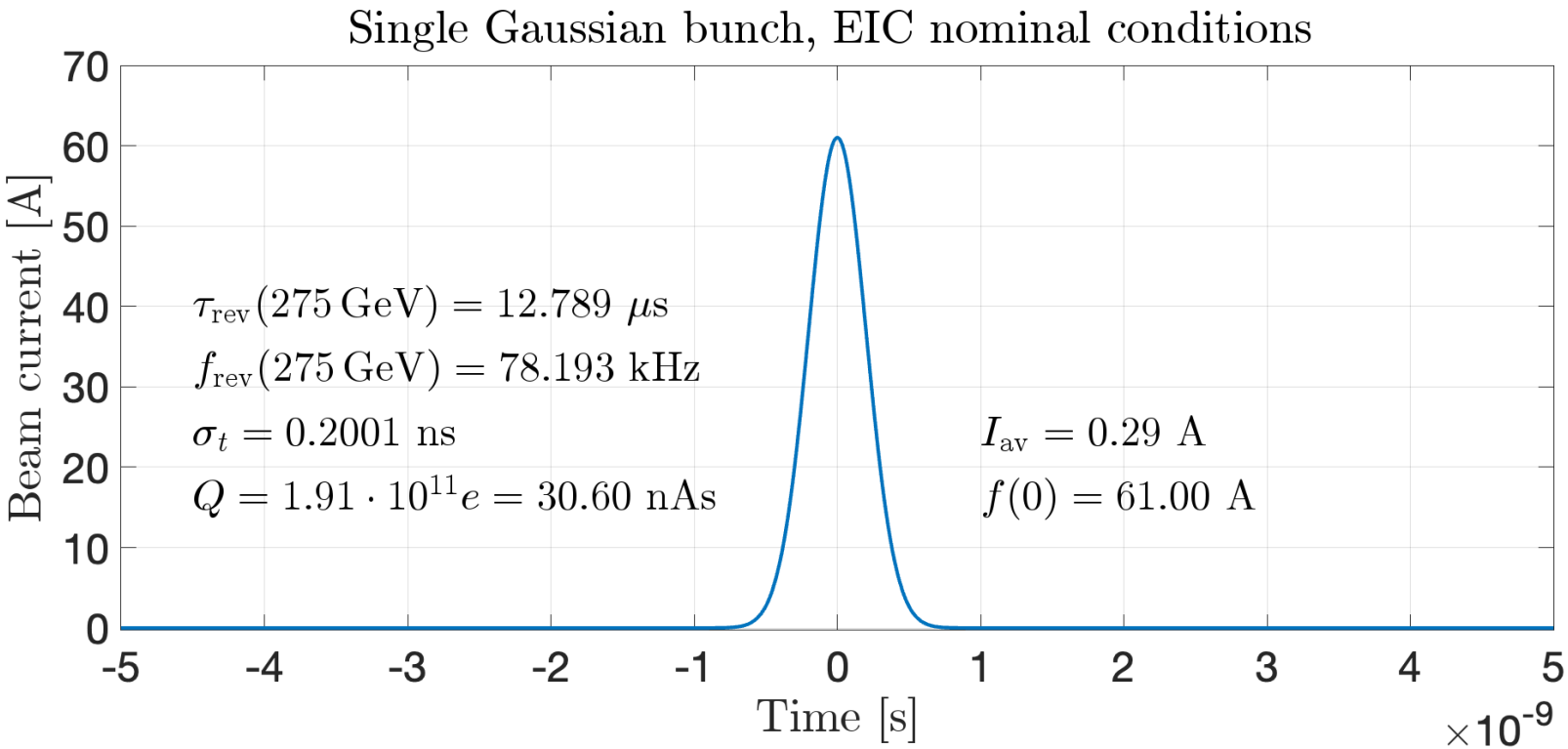

Pulse shape described by

$$f(t) = \frac{Q}{\sqrt{2\,\pi}\sigma_t} \exp\left(-\frac{t^2}{2\sigma_t^2}\right) \tag{12}$$

Bunch structure

EIC situation:

- Time period between two adjacent bunches: $\tau_\mathrm{b} = \frac{\tau_\mathrm{rev}}{N_b} = 10.85\,\mathrm{ns}$
- Number of stored bunches $N_b = 1160$
- Bunch frequency $f_\mathrm{b} = \frac{1}{\tau_\mathrm{b}} = 92.2081\,\mathrm{MHz}$

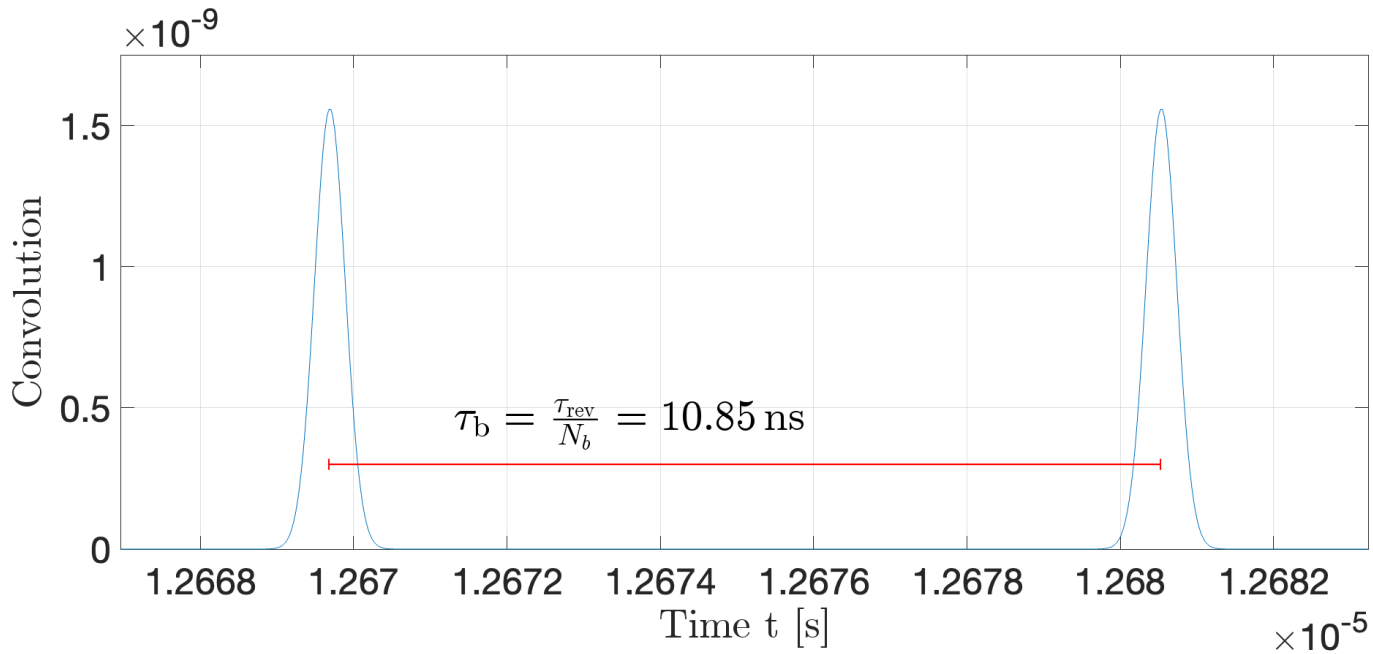

Gaussian convoluted with (finite) series of delta functions

Total beam current as function of time t given by

$$I(t) = \int_{-\infty}^{\infty} f(t-\xi) \sum_{k=-\infty}^{\infty} \delta\left(\xi - k\frac{\tau_{\mathrm{rev}}}{N_{\mathrm{b}}}\right) \mathrm{d}\xi \tag{13}$$

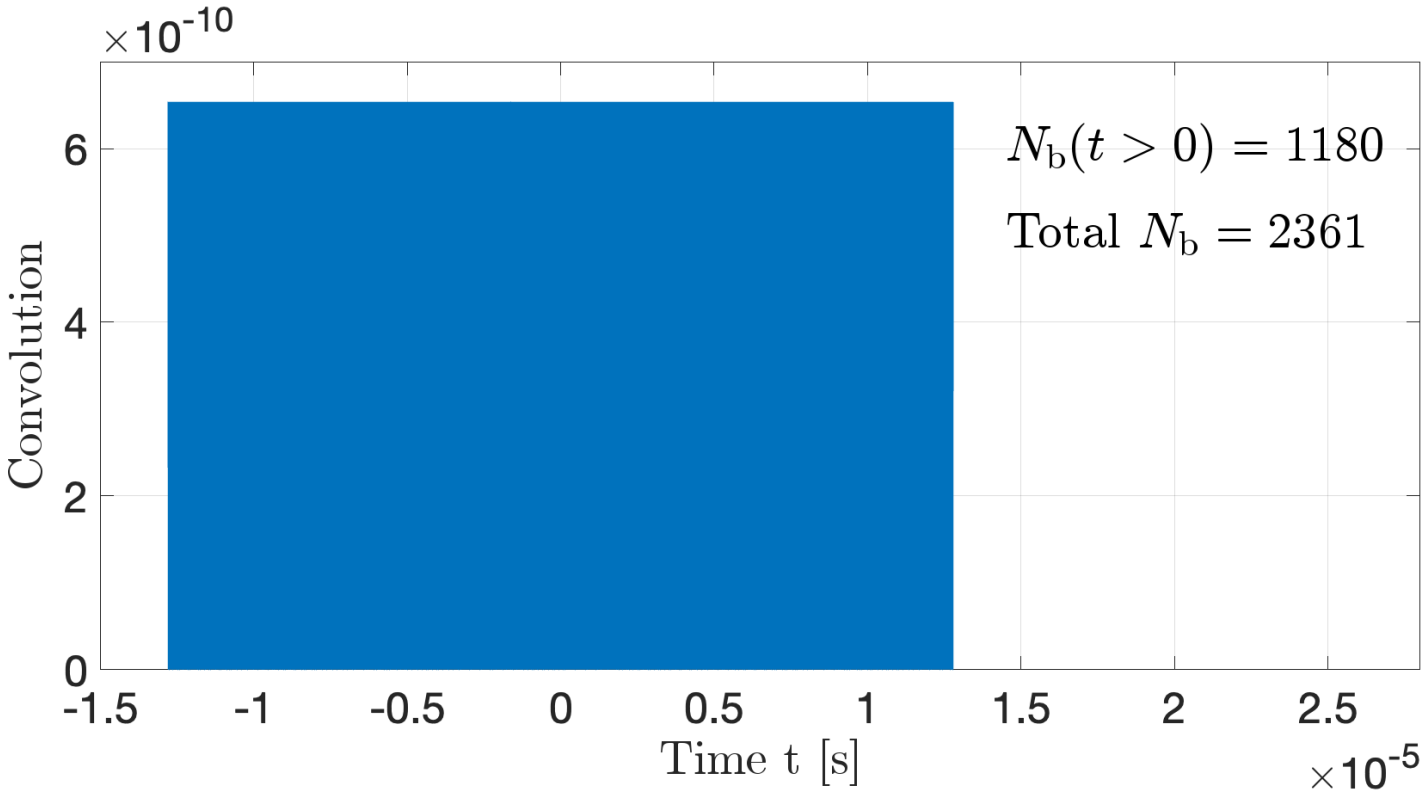

Produced radio-frequency fields

- Single-sided amplitude spectrum of FFT

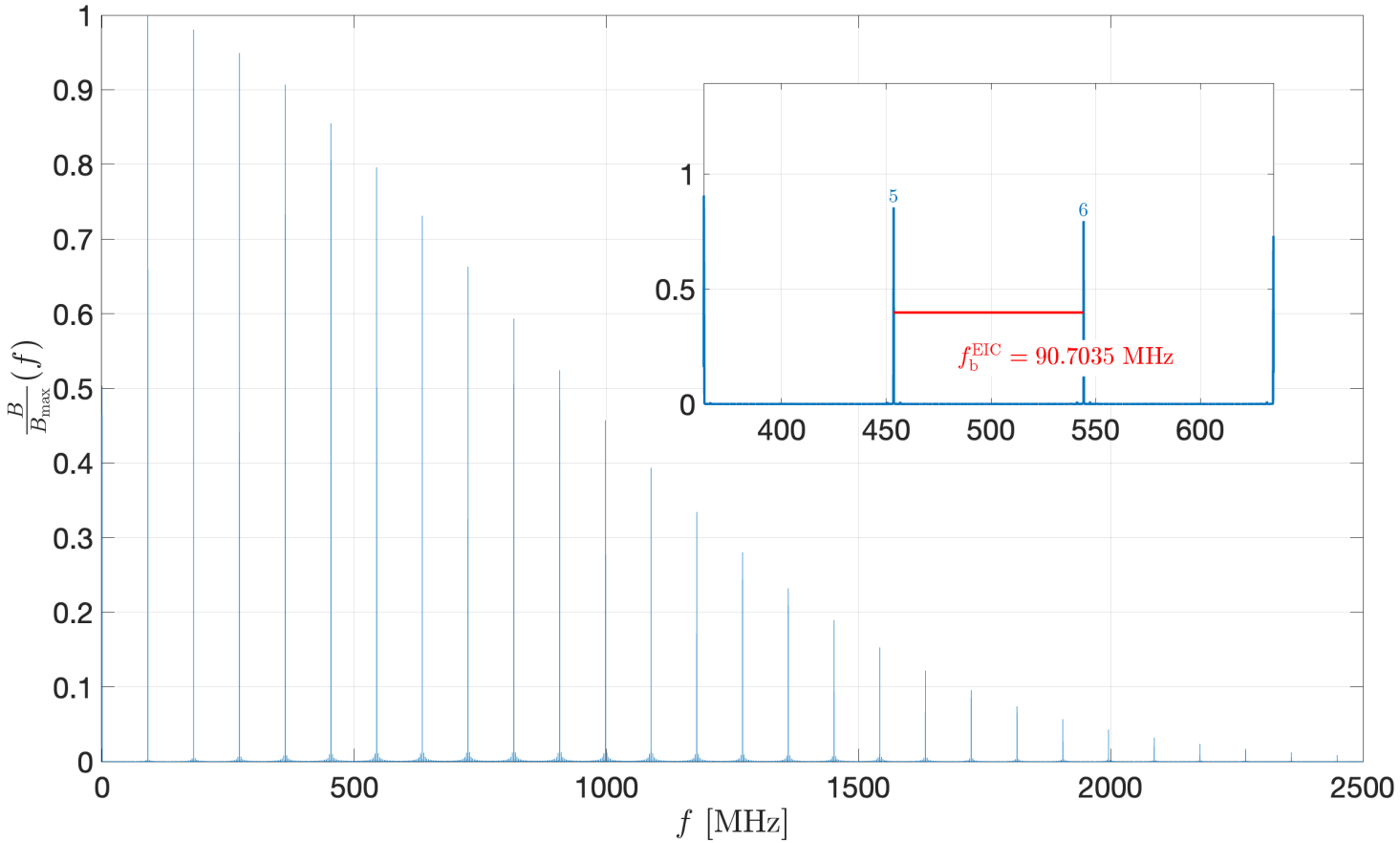

Amplitudes of radio-frequency fields

- Frequency spacing becomes larger at EIC $\Rightarrow$ fewer resonances contribute
- RF field amplitudes at EIC $\approx 10\times$ larger compared to RHIC
  $\Rightarrow$ increased transition probability due more photons ($n_\gamma \propto B^2$).

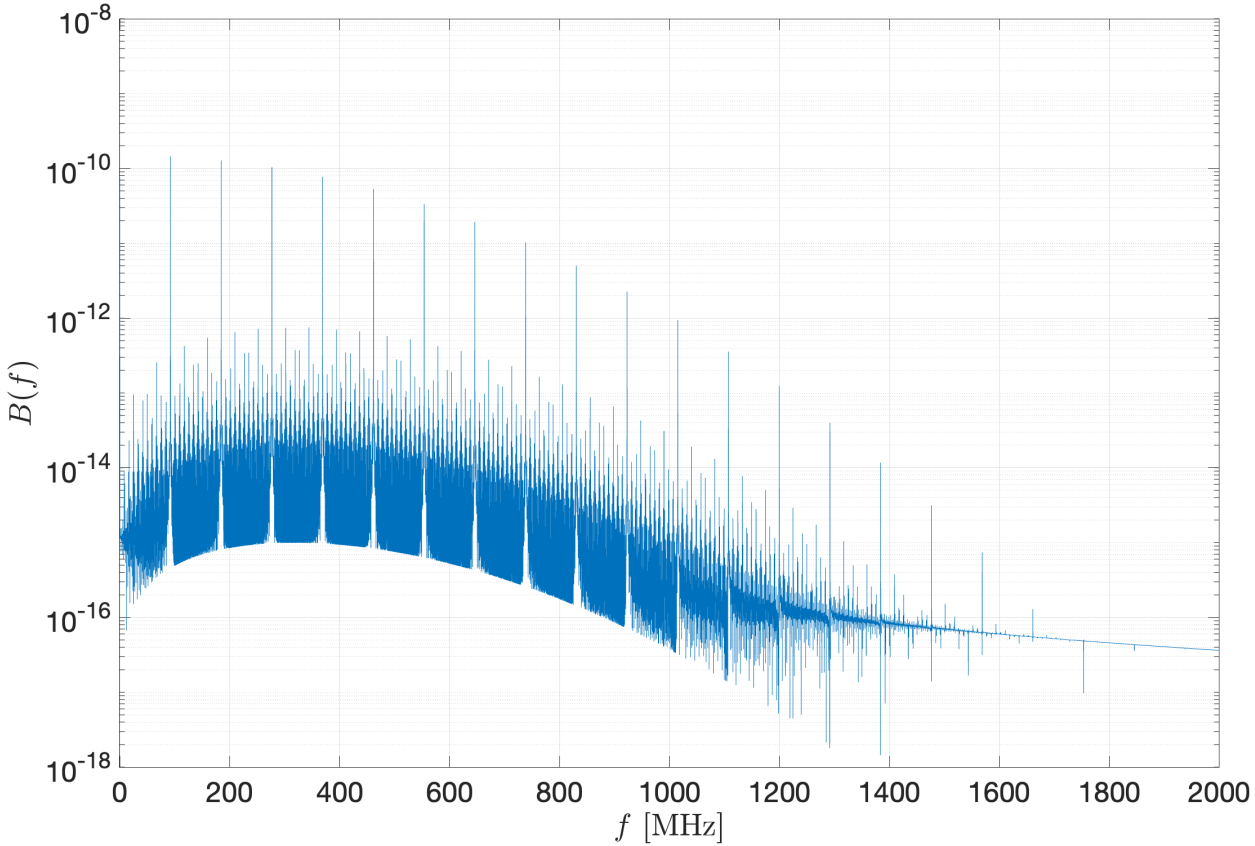

Hyperfine transitions in H from bunch fields at EIC

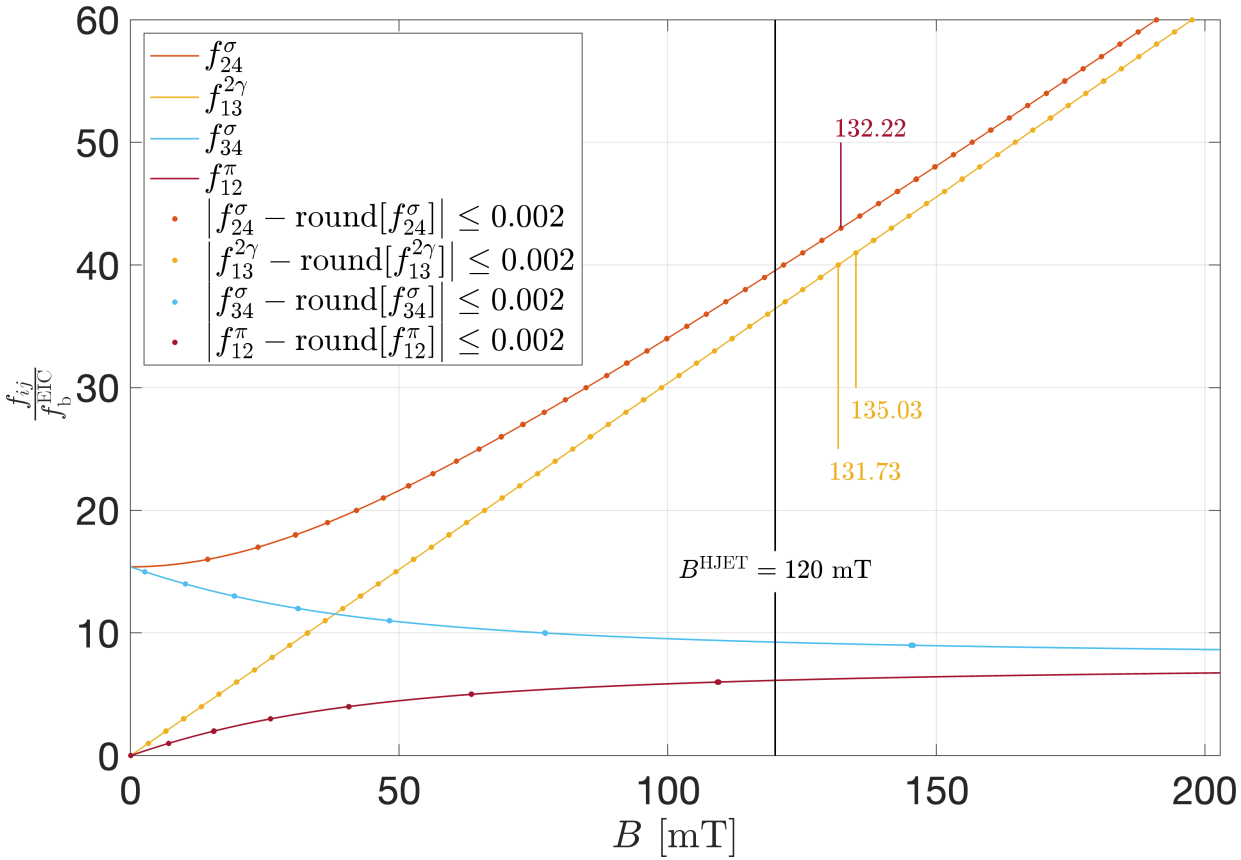

Depolarization (numerically) occurs when

$$\left|\frac{f_{ij}}{f_b^{\mathrm{EIC}}} - n\right| \leq 0.002\,,\ n \in \mathbb{N}$$

In contrast to RHIC, for $B < 200\,\mathrm{mT}$

- **all transitions below harmonic number ≈ 60 contribute at EIC!**

Hyperfine transitions in H from bunch fields at EIC

How about the region of small B?

- At RHIC, this region was inaccessible, as spacing of $f_{13}^{2\gamma} \approx 0.3\,\mathrm{mT}$.
- At EIC, at $\approx 5\,\mathrm{mT}$, spacing of $f_{13}^{2\gamma} \approx 3.3\,\mathrm{mT}$.

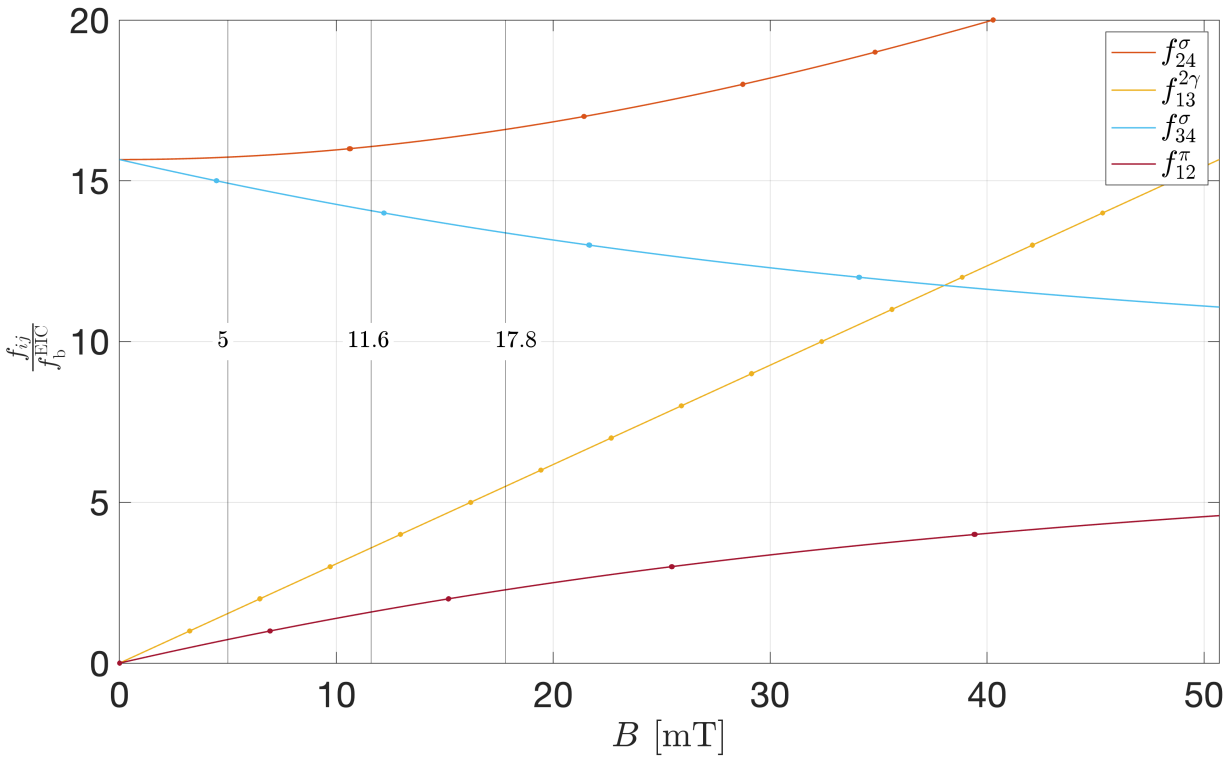

Magnetic field from beam charge

RHIC

Moving charge of beam induces magnetic field at HJET target

- β functions at the HJET in IP12 from G. Robert-Demolaize, 23.07.2024 for RHIC at top energy, determined from fill #34819,

$$\begin{aligned} \beta_x &= 8.243\,\mathrm{m}, \beta_y = 8.326\,\mathrm{m} \\ \beta_x &= 8.303\,\mathrm{m}, \beta_y = 8.252\,\mathrm{m} \end{aligned} \tag{14}$$

- Assume in the following an average $\bar{\beta}_{\mathrm{jet}} = 8.281$
- Since $\beta_x \approx \beta_y$, we deal with a round beam. The normalized RMS emittance taken from the RHIC dashboard during run 24 is:

$$\varepsilon^N_{\mathrm{rms}} = 2.5\,\mu\mathrm{m}\,. \tag{15}$$

Beam parameters for RHIC

- For a Gaussian beam, assume a current density of

$$J = \frac{I(t)}{2\pi\sigma_r^2} \exp\left(-\frac{r^2}{2\sigma_r^2}\right), \quad \text{where} \quad \sigma_r = \sqrt{\frac{\bar{\beta}_{\text{jet}}\epsilon_{\text{rms}}^{\text{N}}}{k \cdot \beta\gamma}} \tag{16}$$

- Due to symmetry of problem, magnetic field $\vec{B}$ will be tangential to concentric circles around z-axis. Thus, $\vec{B}$ can be written as

$$\vec{B} = B(r)\vec{e}_\phi \tag{17}$$

- With beam traveling in $\vec{e}_z$ direction, the integration for a cylindrical Gaussian beam yields flux density

$$\vec{B}(r) = \frac{\mu_0 I(t)}{2\pi r}\left[1 - \exp\left(-\frac{r^2}{2\sigma_r^2}\right)\right]\vec{e}_\phi \text{ , with } \vec{e}_\phi = \vec{e}_z \times \vec{e}_r \tag{18}$$

-

Emittance[2]	Beam width	injection 23.5 GeV	flattop 250 GeV
$\epsilon_{\text{rms}}^N = 2.5\,\mu\text{m}$	$\sigma_r^{1\sigma} = \left(\bar{\beta}_{\text{jet}} \cdot \frac{\epsilon_{\text{rms}}^N}{\beta\gamma}\right)^{\frac{1}{2}}$	0.89 mm	0.28 mm
$\epsilon_{95}^N = \epsilon_{\text{rms}}^N \cdot 5.993$	$\sigma_r^{95} = \sigma_r^{1\sigma} \cdot \sqrt{5.993}$	2.18 mm	0.68 mm

[2] Factor 5.993 to convert 1D rms emittance to emittance for 95% of particles in a beam [8].

Magnetic field from beam charge at RHIC

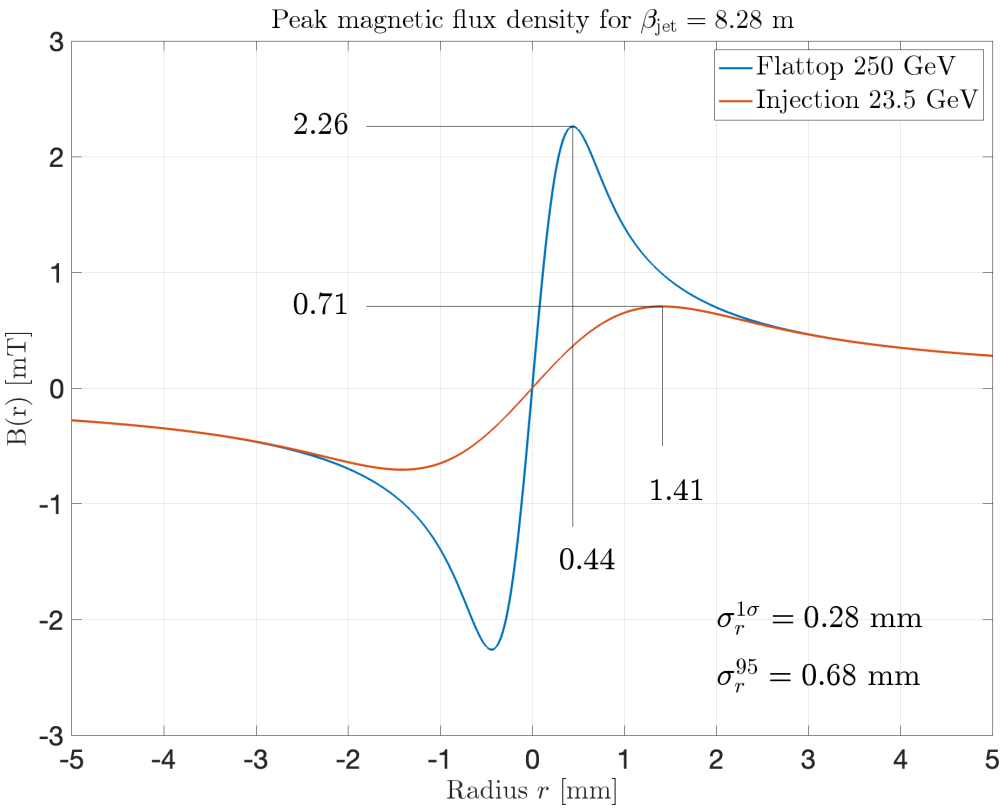

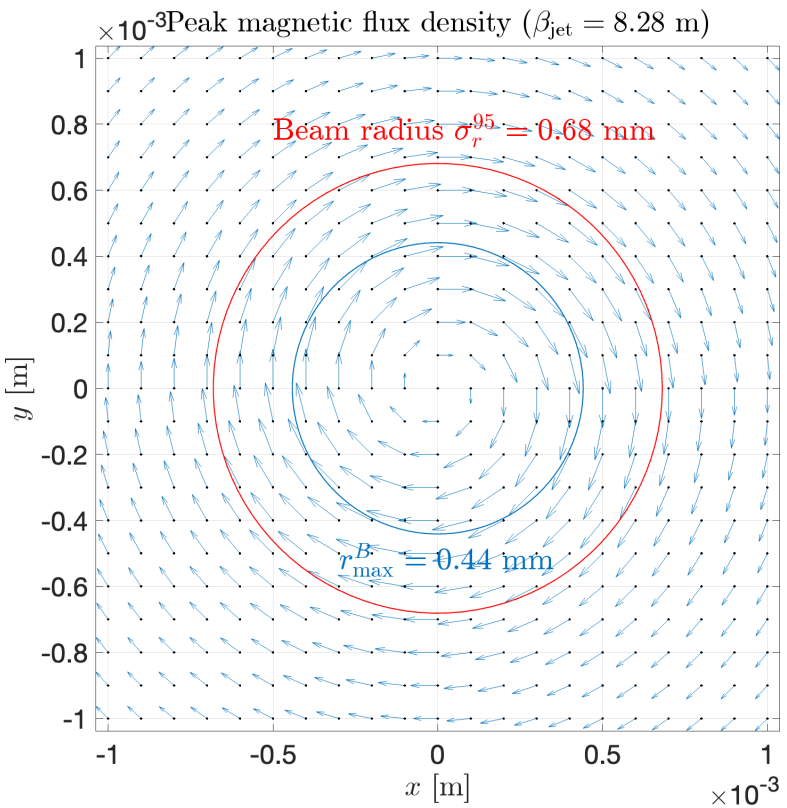

Effect of induced magnetic field on jet pol at RHIC

- Systematic variation of magnetic holding field in region struck by beam:
- In center ($r = 0$), $|\vec{B}(r)| = B_y^{\text{nom}} = 120\,\text{mT}$
- Inside beam, magnetic fields are modified

$$\frac{\int_0^{\sigma_r^{95}} B(r)\mathrm{d}r}{\sigma_r^{95}} = 1.73\,\text{mT} \tag{19}$$

- In midplane ($y = 0$), still $\vec{B} \parallel \vec{e}_y$.
  - Left hemishere: $\bar{B}^{\text{L}} = 121.73\,\text{mT}$, Right hemishere: $\bar{B}^{\text{R}} = 118.27\,\text{mT}$

  Relative change of target polarization inside beam is, e.g.,

$$\delta P = \frac{P_{|1\rangle+|4\rangle}(\bar{B}^{\text{L}}) - P_{|1\rangle+|4\rangle}(\bar{B}^{\text{R}})}{P_{|1\rangle+|4\rangle}(B_y^{\text{nom}})} \leq 0.21\% \tag{20}$$

- In vertical plane ($x = 0$), $\vec{B} \nparallel \vec{e}_y$.

Conclusion for RHIC

- No depolarization due to variation of B inside beam (slide 24)
- Effect small/tolerable in terms of syst. contribution to jet polarization

Beam parameters

EIC

EIC beam parameters taken from Conceptual Design Report [9]

- 275 GeV
- β-functions:
  - $\beta_x = 230.323\,\mathrm{m}$
  - $\beta_y = 69.935\,\mathrm{m}$
  - $\rightarrow$ assumed in the following: $\bar{\beta} \approx 150\,\mathrm{m}$ for future location of HJET at IP4 (from H. Lovelace, 31.07.2024).
- Like before, $\epsilon^N_{95} = \epsilon^N_{\mathrm{rms}} \cdot 5.993$
- Two situations for IP4:

Beam	$\epsilon^N_{\mathrm{rms}}$ [μm]	$\sigma_r^{1\sigma}$ [mm]	σ_r^{95} [mm]
uncooled	2.5	1.13	2.76
cooled	0.47	0.49	1.20

Magnetic field from beam charge

EIC

Uncooled beam

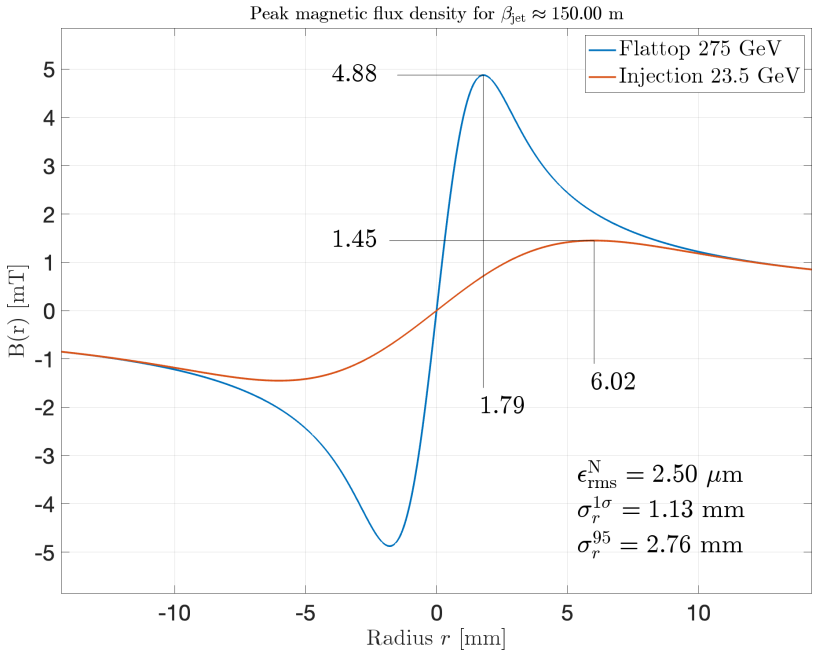

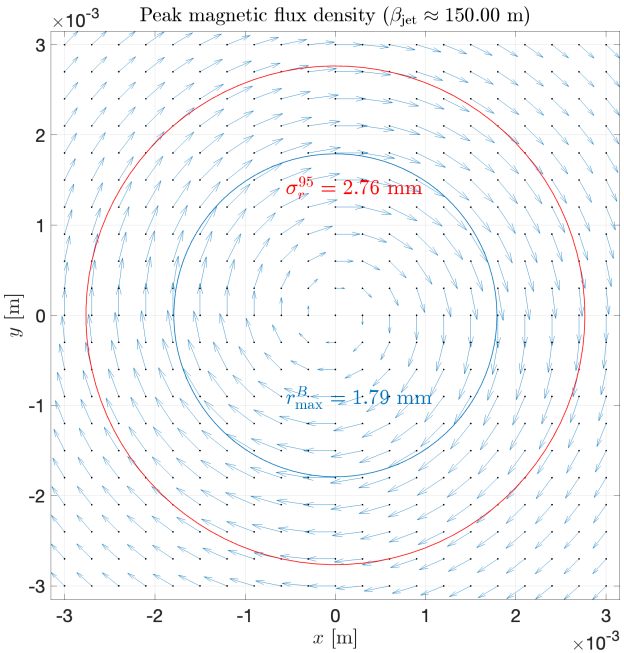

HJET beam size

- On flattop, transverse dimensions of uncooled proton beam at IP4 comparable to HJET beam diameter (6 mm FWHM $\rightarrow \sigma^{\mathrm{HJET}} \approx 2.55$ mm).

Magnetic field from beam charge

EIC

Cooled beam

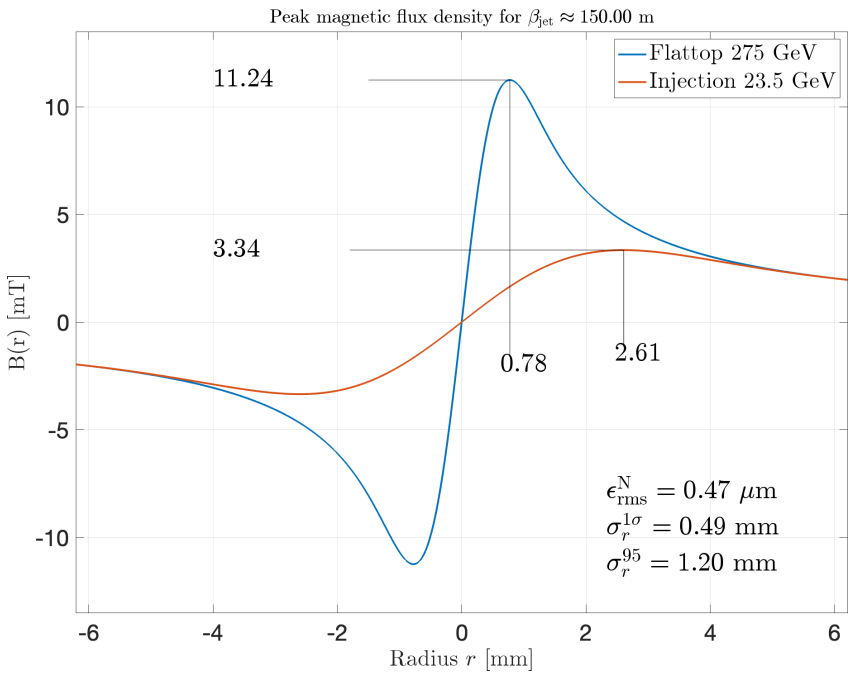

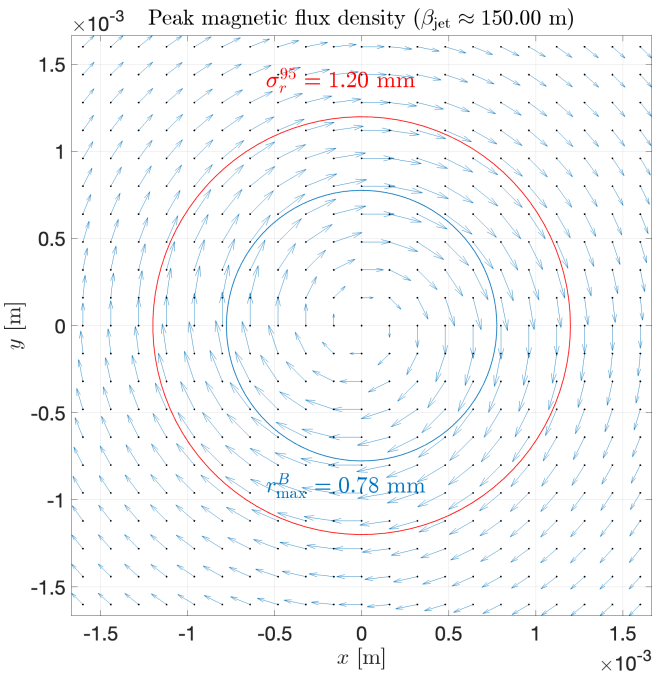

Effect on magnetic field at jet target and its polarization

EIC

Implications for EIC

1. Induced B field from beam charge:
   - uncooled beam: $B(r) \leq 4.88\,\mathrm{mT}$
   - cooled beam: $B(r) \leq 11.74\,\mathrm{mT}$

   $\rightarrow$ kills idea to apply weak holding field (20 mT) at target (slide 31)
2. Variation of polarization inside target area at 120 mT [Eq. (20)]:
   - uncooled beam: $\delta P = 0.45\%$
   - cooled beam: $\delta P = 1.05\%$
3. Variation of polarization inside target area at 300 mT [Eq. (20)]:
   - uncooled beam: $\delta P = 0.1\%$
   - cooled beam: $\delta P = 0.1\%$
4. **Due to fields induced by beam charge (item 1), beam-induced depolarizing resonances appear in HJET target** (slide 30)

Mitigation of beam-induced magnetic field effect at EIC

Possible solutions

1. At RHIC, B-field was moved to $\approx 120\,\mathrm{mT}$ and $\frac{f_{ij}}{f_b^{\mathrm{RHIC}}} \geq 350$ ignored (slide 24)
2. **Strategy for EIC: $\Rightarrow$ push harmonics to ≥ 100 $\Rightarrow$ holding field $\geq 350\,\mathrm{mT}$**

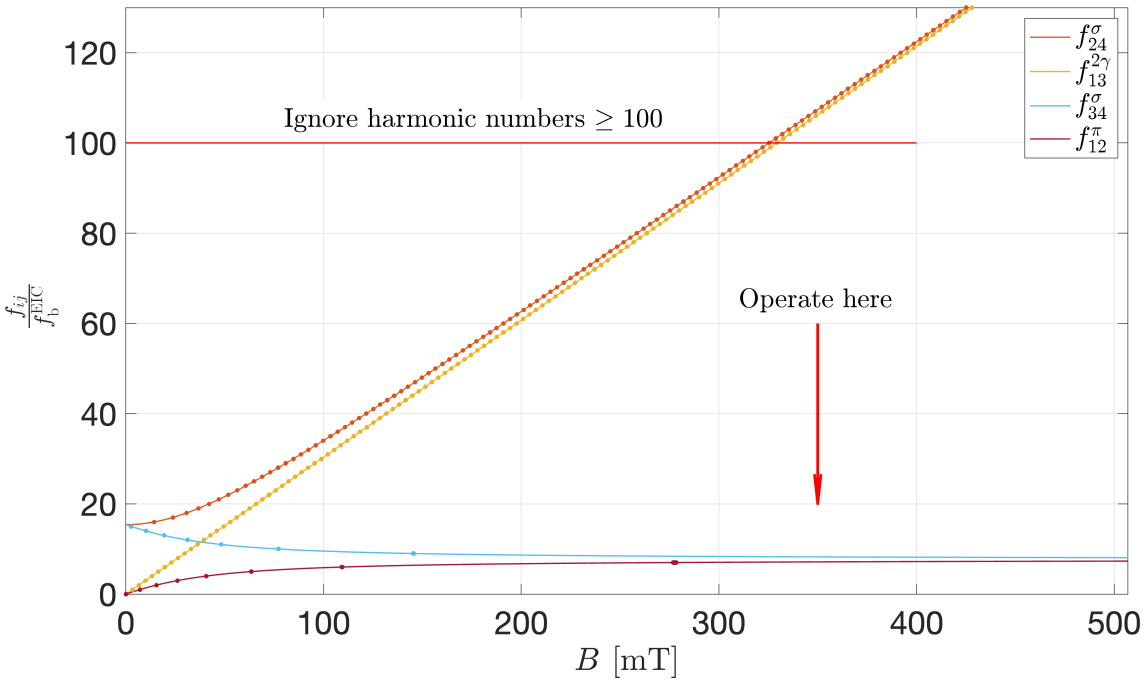

Where exactly is cutoff located for f_{24}^{σ} and $f_{13}^{2\gamma}$?

- What is know from RHIC or can still be learned about at which B harmonics become harmless?

Concept for magnetic guide field for HJET at EIC

But first ...

Spin-dependent *pp* elastic cross section (spin 1/2 + spin 1/2)

With polarized beam $\vec{P}$ and polarized target $\vec{Q}$, all components of $\vec{P}$ can be determined from spin-dependent cross section, as shown in Table below [10, 11]:

$$\begin{aligned}\sigma/\sigma_0 = 1 &+ A_y \left[(P_y + Q_y)\cos\phi - (P_x + Q_x)\sin\phi\right] \\ &+ A_{xx}\left[P_x Q_x \cos^2\phi + P_y Q_y \sin^2\phi + (P_x Q_y + P_y Q_x)\sin\phi\cos\phi\right] \\ &+ A_{yy}\left[P_x Q_x \sin^2\phi + P_y Q_y \cos^2\phi - (P_x Q_y + P_y Q_x)\sin\phi\cos\phi\right] \\ &+ A_{xz}\left[(P_x Q_z + P_z Q_x)\cos\phi + (P_y Q_z + P_z Q_y)\sin\phi\right] + A_{zz} P_z Q_z\end{aligned}$$

- Full angular distributions of all A_{ik}'s were determined.
- Single input: $A_y = 0.2122 \pm 0.0017$ at $\theta_{\text{lab}} = 8.64° \pm 0.07°$ [12], known from $A_y = 1$ point in $p + {}^{12}\text{C}$ elastic scattering [13].

Most importantly in context

- determination of beam $\vec{P} = (P_x, P_y, P_z)$ and target $\vec{Q} = (Q_x, Q_y, Q_z)$, as well as non-flipping components possible (slide 72)

Spin-dependent *pp* elastic cross section

The above is relevant for two reasons

1. The spin-dependence of $\vec{p}\vec{p}$ elastic scattering allows to reconstruct angular distributions of all (in that case five) polarization observables.
2. With suitable magnetic guide field, target polarization $\vec{Q}$ can be oriented along any direction, for instance along x, so that $\vec{Q} = Q \cdot \vec{e}_x = \vec{Q}_x$
   - Absolute value of target polarization Q determined by BRP

Two things needed to port HJET from RHIC to EIC with $\frac{\Delta P}{P} \leq 1\%$

1. Substantially stronger holding field of $|\vec{B}| \approx 300$ to 350 mT than at RHIC
2. Detector capable to pick up azimuthal asymmetries $\propto \sin\phi$ and $\propto \sin 2\phi$ (slide 71)
   - foresee proper detector symmetry to provide $\vec{d}\vec{d}$ beam absolute polarimetry, i.e., beyond $\propto \sin 2\phi$.

Holding field system for $|\vec{B}| \approx 0.3\,\mathrm{T}$ with $\vec{B} \parallel \vec{e}_{x,y,z}$

Work together with Helmut Soltner (FZJ, Germany)

Motivation:

- Reconcile strong magnetic holding field with open detector geometry to determine, e.g., all spin components of beam polarization $\vec{P} = (P_x, P_y, P_z)$
- Exploit magnetic moments $\vec{m}$ of homogeneously magnetized spheres [14–16]
- Invert $\vec{m}$ in vacuum to reverse $\vec{B}(O)$
- Reorient $\vec{m}$'s to generate $\vec{B}(O) \parallel \vec{e}_{x,y,z}$

Consider two sets of frames

- Set 1:
  - Interaction region where beam meets atoms at (O)
  - Set 1: $100\,\mathrm{mm}_x \times 100\,\mathrm{mm}_y \times 40\,\mathrm{mm}_z$ and
    Set 2: $100\,\mathrm{mm}_x \times 100\,\mathrm{mm}_y \times 110\,\mathrm{mm}_z$, centered around x, y, and z axes.
  - 8 permanently magnetized spheres in each corner of each frame:
    - NeFeB magnets provide remanence of $B_r = 1.49 - 1.55\,\mathrm{T}$ (type N58)
    - Radius $r = 30\,\mathrm{mm}$

Holding field system: Calculation

Calculation

- Flux density vector as function of $\vec{m}$ in space

$$\vec{B}(\vec{r}) = \frac{\mu_0}{4\pi}\left[\frac{3\left(\vec{m}\cdot\hat{R}\right)\hat{R}-\vec{m}}{|R|^3}\right], \tag{21}$$

  where $\vec{R} = \vec{r} - \vec{r}_0$, $\hat{R} = \frac{\vec{R}}{|R|}$.

- Optimize orientation of $\vec{m}$'s to maximize $\vec{B}(O)$ in x, y, and z direction:
  - maximize dot product $\vec{m}\cdot\hat{R}$ and set $m_y = 0$, to obtain, e.g., max. B_y.

Component $B_x(O)$ using two sets of $\vec{m}$'s

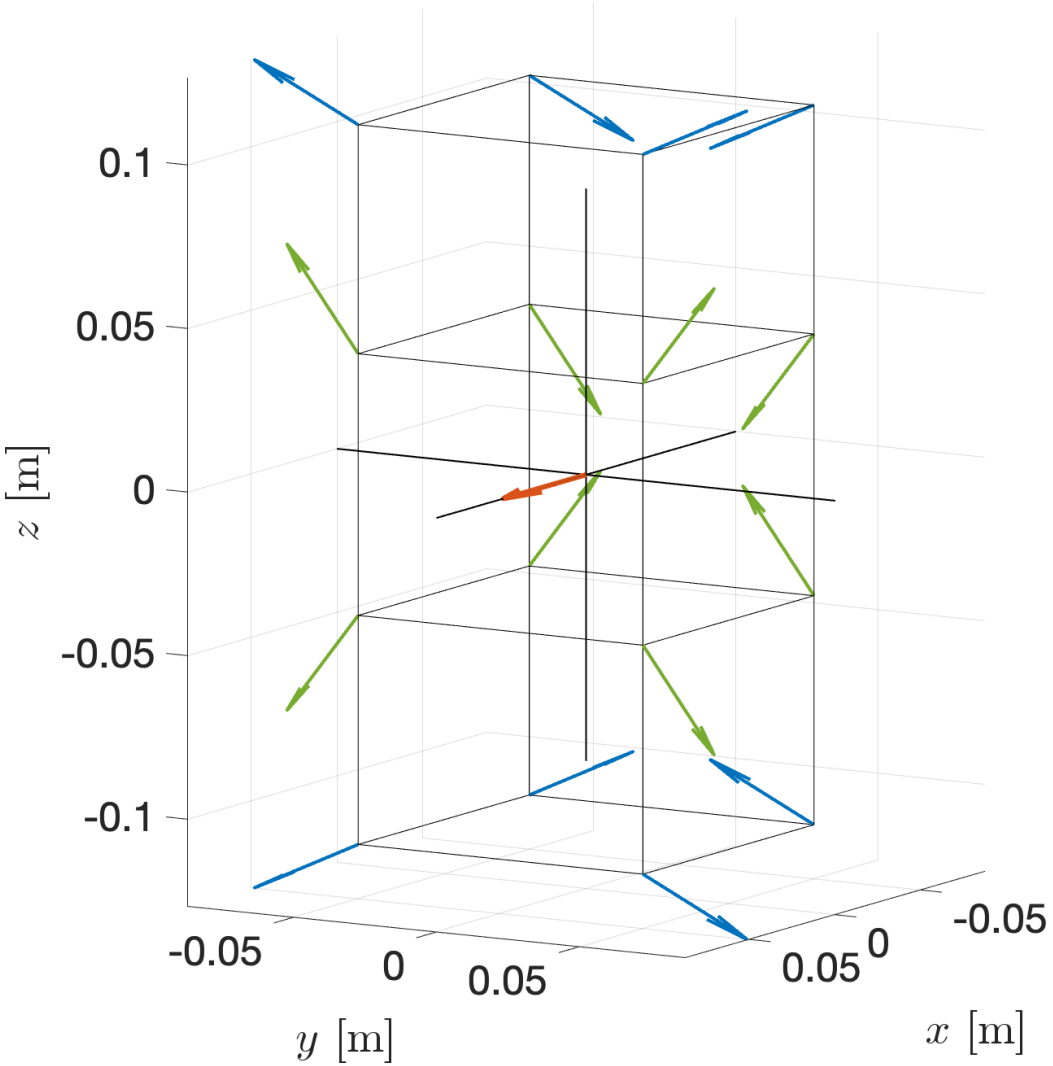

$$B_x: \begin{pmatrix} 0.3224 \\ 0 \\ 0 \end{pmatrix} \text{T}$$

Component $B_y(O)$ using two sets of $\vec{m}$'s

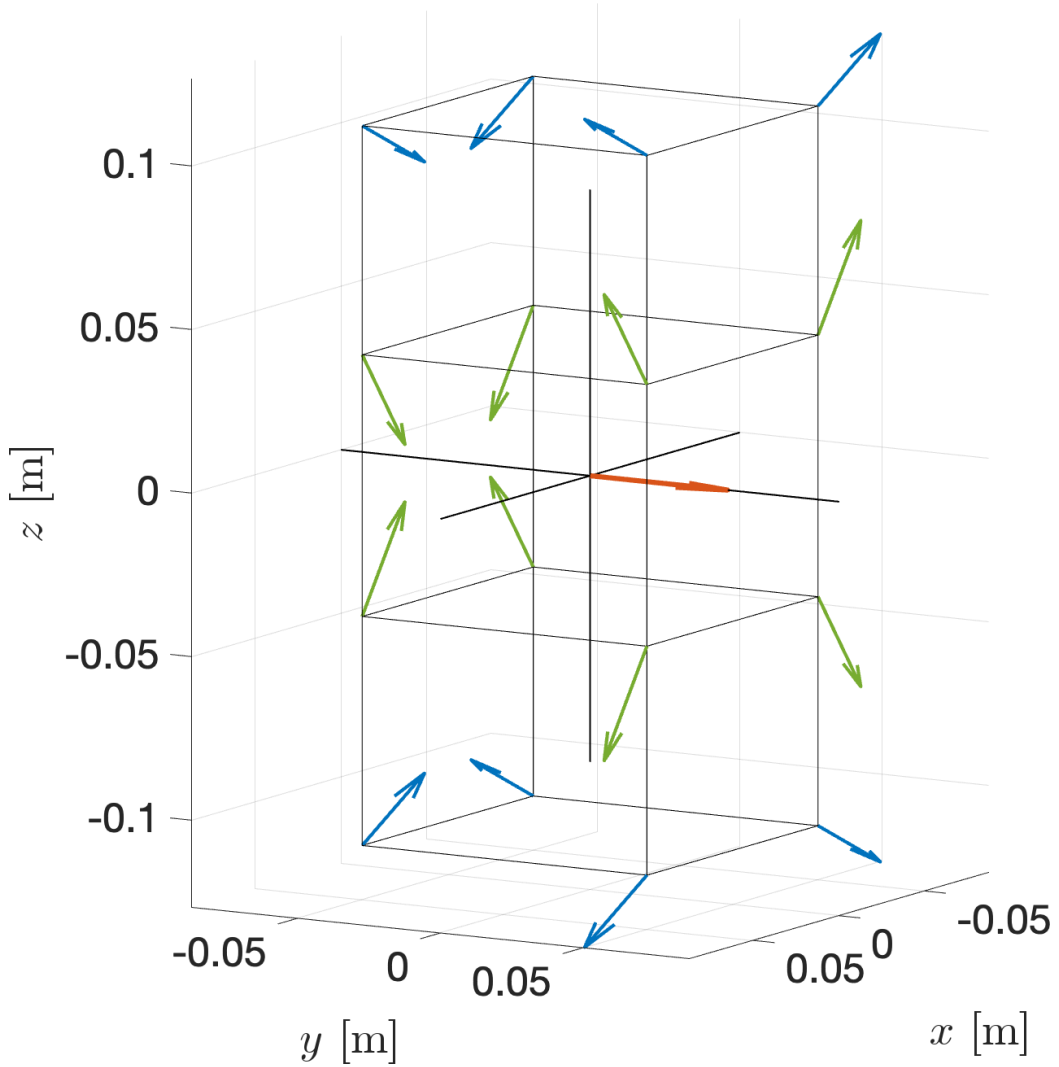

$$B_y: \begin{pmatrix} 0 \\ 0.3224 \\ 0 \end{pmatrix} \text{T},$$

Component $B_z(O)$ using two sets of $\vec{m}$'s

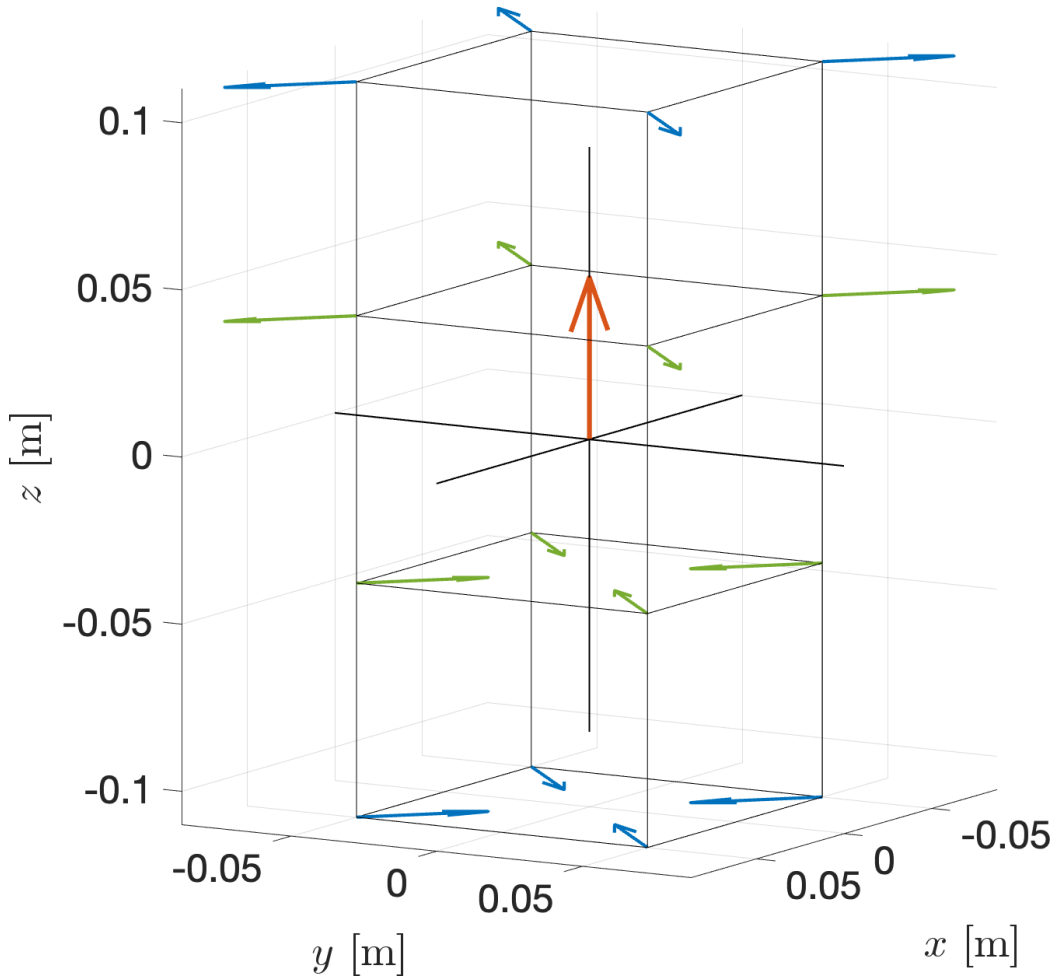

$$B_z: \begin{pmatrix} 0 \\ 0 \\ 0.3227 \end{pmatrix} \text{T}$$

Technical realization

With properly rotated spheres

- Setup allows for azimuthally symmetric detector setup with acceptance $\Delta\phi \approx \pm 15^\circ$ at $\phi = 45$, 135, 225, and 315°
  - $\phi = \arctan(30/50) = 31^\circ$
- **Technical challenges:**
  1. Accurate reorientation of magnetized spheres in vacuum
  2. Vacuum compatible coatings, like Ni, or stainless steel covers to prevent H and H_2 from deteriorating NeFeB
  3. **First Step: build a lab test setup and verify concept is technically sound**

Force and torque between two dipoles $\vec{m}_1$ and $\vec{m}_2$ I

Potential energy of magnetic dipole

$$U = -\vec{m} \cdot \vec{B}$$
$$\vec{F} = -\vec{\nabla} U \quad \rightarrow \quad F_{12} = \vec{\nabla}\left(\vec{m}_2 \cdot \vec{B}_1\right) \tag{22}$$

- $\vec{B}_1$ is flux density produced by $\vec{m}_1$ at location of $\vec{m}_2$.

Force:

$$\vec{F}_{12}(\vec{r}_{12}, \vec{m}_1, \vec{m}_2) = \frac{3\mu_0}{4\pi r_{12}^4}\Big[\vec{m}_2\left(\vec{m}_1 \cdot \vec{e}_{12}\right) + \vec{m}_1\left(\vec{m}_2 \cdot \vec{e}_{12}\right) + \vec{e}_{12}\left(\vec{m}_1 \cdot \vec{m}_2\right) - 5\vec{e}_{12}\left(\vec{m}_1 \cdot \vec{e}_{12}\right)\left(\vec{m}_2 \cdot \vec{e}_{12}\right)\Big] \tag{23}$$

- $\vec{r}_{12}$ is vector between $\vec{m}_1$ and $\vec{m}_2$, $\vec{e}_{12} = \frac{\vec{r}_{12}}{|r_{12}|}$.

Torque

$$\vec{\tau} = \vec{m}_2 \times \vec{B}_1 \tag{24}$$

Force and torque between two dipoles $\vec{m}_1$ and $\vec{m}_2$ II

Examples: $\vec{m}_1 \perp \vec{m}_2$

1. Spheres touch:

$$r_{12} = 0.06\,\mathrm{m} \quad \vec{F}_{12} = -417\,\mathrm{N} \quad \tau_{12} = 8.3\,\mathrm{Nm} \tag{25}$$

2. System assembled:

$$r_{12} \geq 0.07\,\mathrm{m} \quad \vec{F}_{12} \leq -225\,\mathrm{N} \quad \tau_{12} = 5.2\,\mathrm{Nm} \tag{26}$$

Flux density of system in 3D

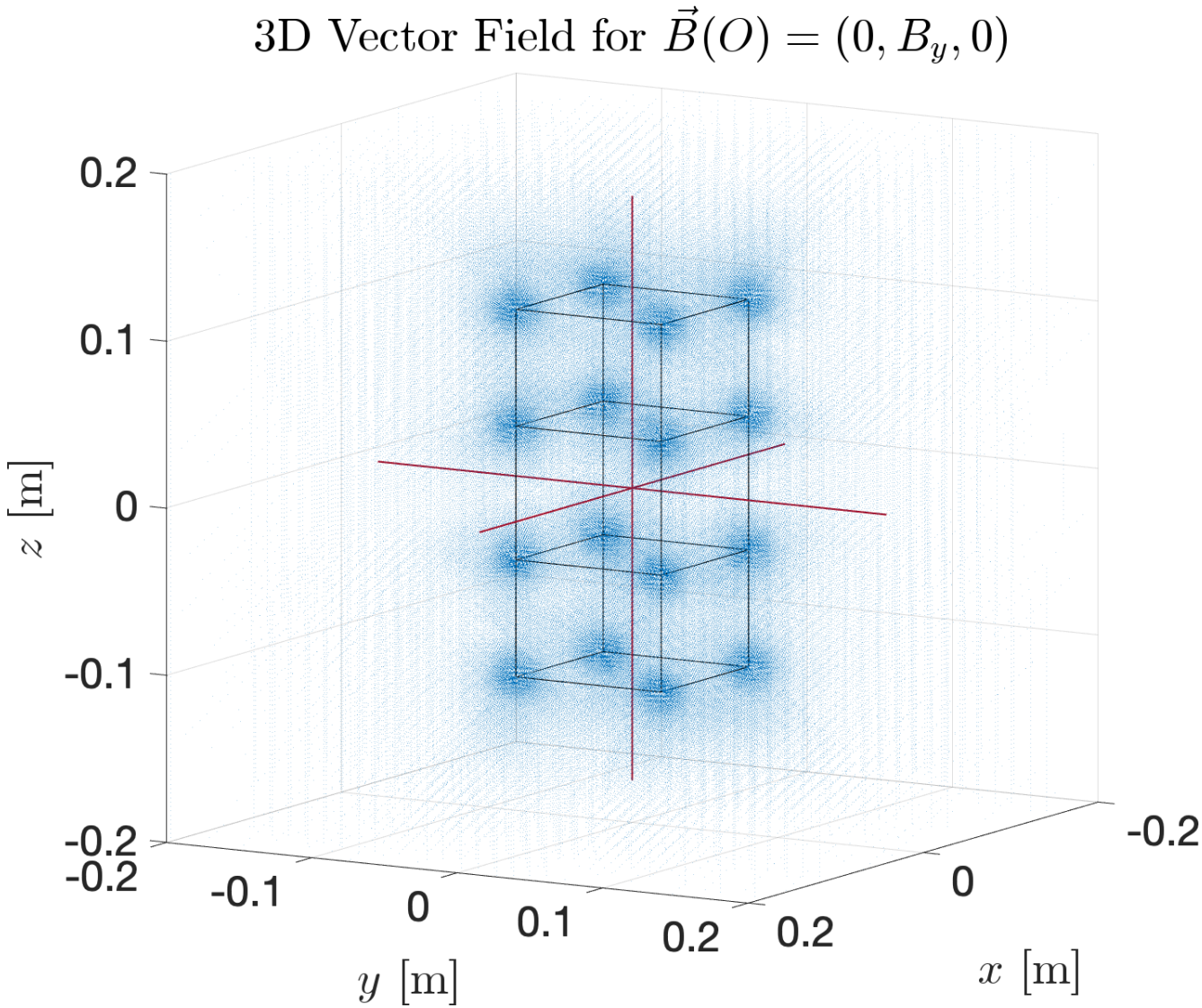

No zero crossings along axes

$\vec{B}(O) \parallel \vec{e}_x$

$\vec{B}(O) \parallel \vec{e}_y$

$\vec{B}(O) \parallel \vec{e}_z$

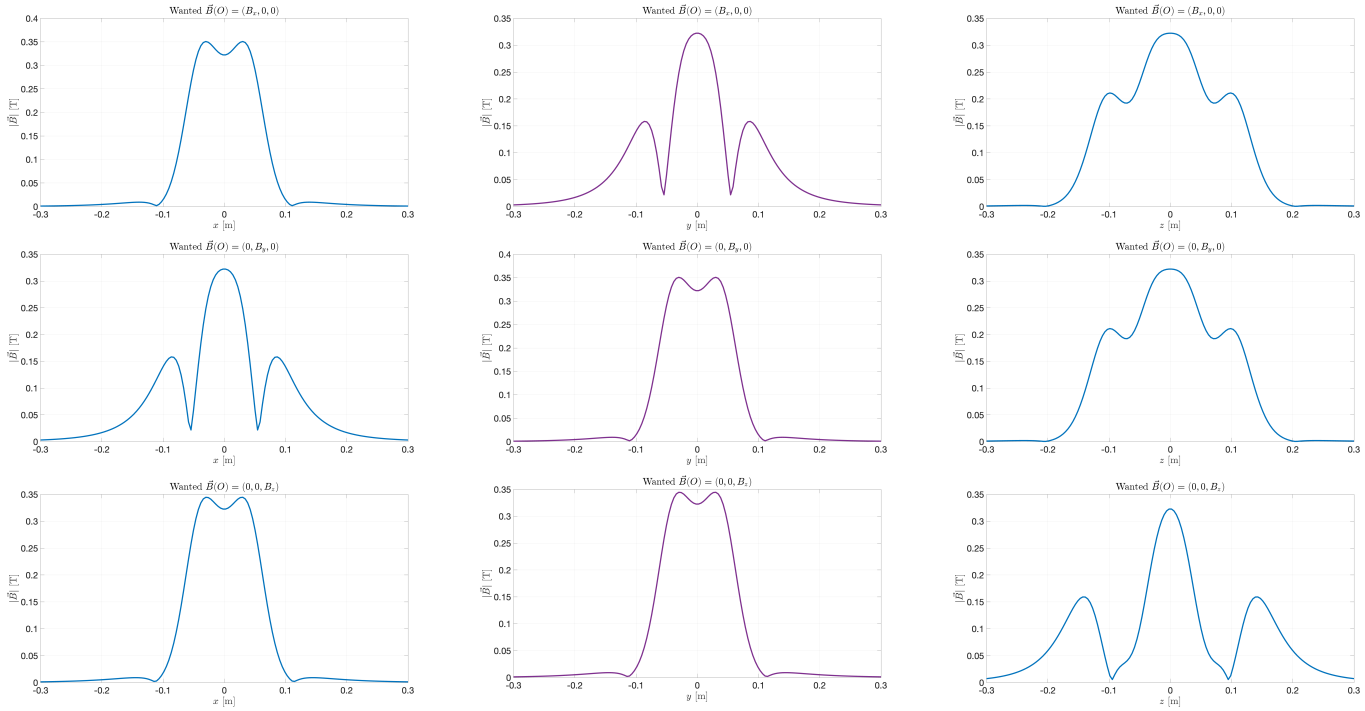

x y z

- No zero crossing of magnetic field along vertical jet (y) axis
- $B_y^{\min} \approx 1.9\,\mathrm{mT}$ sufficient to avoid Majorana depolarization
- Field integrals along beam (z) axis

$\vec{B}(O)$	$\parallel \vec{e}_x$	$\parallel \vec{e}_y$	$\parallel \vec{e}_y$
$\int \lvert\vec{B}\rvert \mathrm{d}z$	0.0667 Tm	0.0667 Tm	0.0546 Tm

Polarized $^3\vec{\text{He}}$ Atomic Beam Source

Original MIT development for nEDM exp't at Oakridge

- Prajwal T MohanMurthy, J. Kelsey, J. Dodge, R. Redwine, R. Milner, P. Binns, B. O'Rourke
- nEDM discontinued

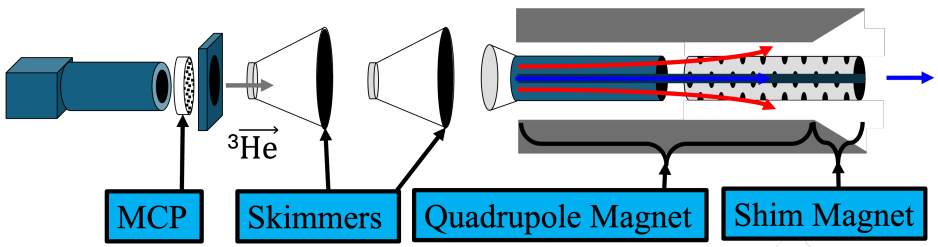

$^3\vec{\text{He}}$: quadrupole magnet selects spins
- **1.3 K ≈ 86 μeV**
- $\Delta E = \mu_m \approx 67$ neV/T
- initial angle very important

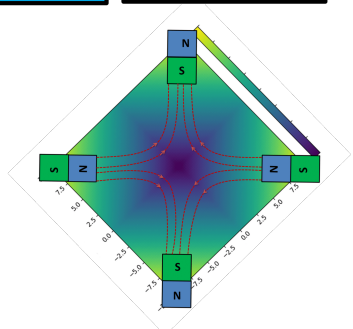

High flux device

- $\geq 1 \times 10^{14}$ atoms/s $\rightarrow$ $d_t \geq 1 \times 10^{13}$ atoms/cm^2
- an ideal device for absolute $^3\vec{\text{He}}^{++}$ beam polarimetry at EIC

Absolute polarimetry of $\vec{d}$ beams

Polarized atomic deuterium jet

- Atomic beam sources efficiently produce beams of deuterium atoms
- Ideal would be the use of dual-function RF transition units for $\vec{\text{H}}$ and $\vec{\text{D}}$ atoms
- With vector and tensor polarization accurately determined by BRP, absolute beam polarimetry based on $\vec{d}\vec{d}$ elastic scattering becomes possible
  - + reconstruction of 3D polarization vector, including tensor components.

Polarimetry section at IP4

Carbon, polarized H and ^{3}He gas targets

- Important to set up all polarimeters in one place without much drift, magnetic elements, etc, to minimize spin rotation between them

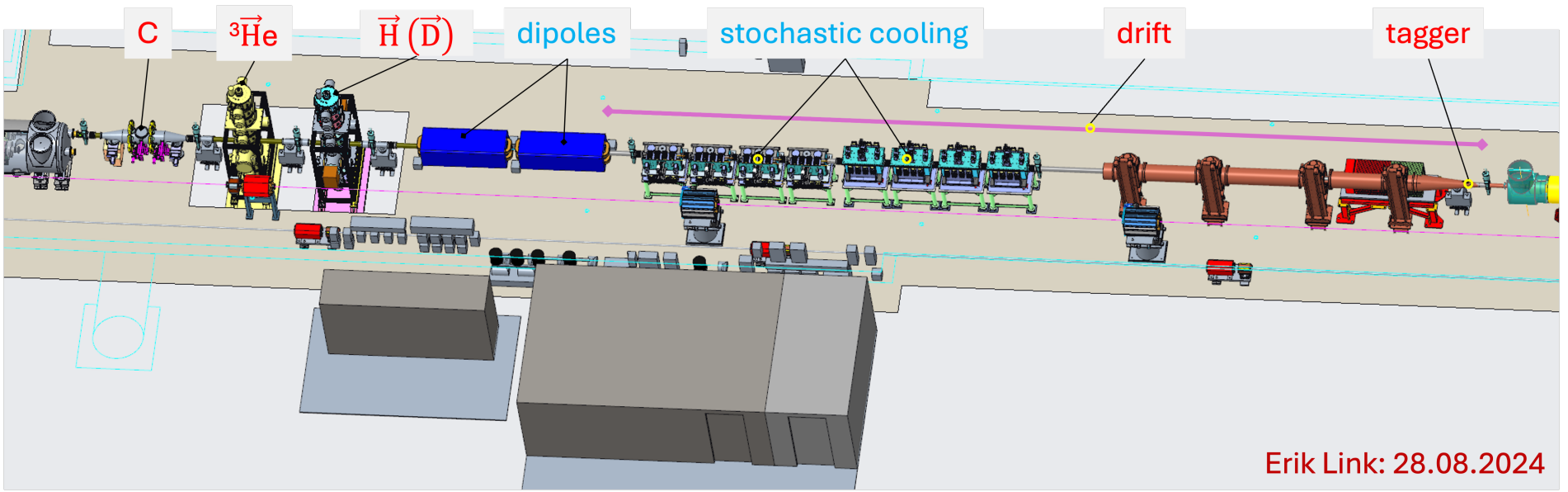

Will carbon fiber targets survive at EIC?

Target heating calculated according to Peter Thieberger

- With proper beam sizes, there is not much difference between RHIC and EIC.
- But, RF heating of the targets not included, will be more severe at EIC due to shorter bunches.
- RF design of target holders needs to be optimized.

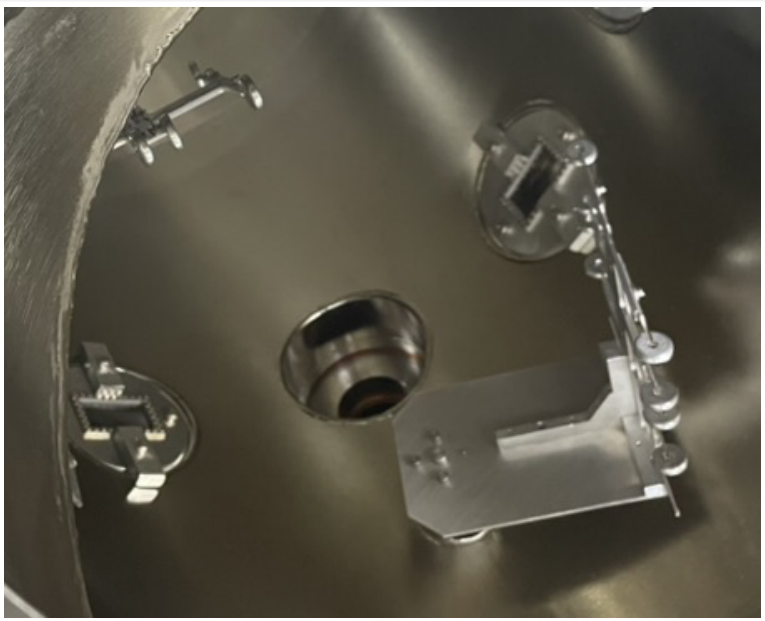

Carbon target temperatures from Thieberger's estimate

RHIC typical conditions

- 111 bunches
- 16×10^{10} protons per bunch
- $\sigma_r^{95} = 0.68\,\text{mm}$

TARGET	GRAPHITE	TUNGSTEN	CARBON
Density (g/cc)	2.26	19.3	2.26
LET (MeV cm^2/g)	1.76E-03	1.12E-03	6.33E-04
Thermal conductivity [W/(K * m)]	390	173	390
Emissivity	0.8	0.35	0.8
Specific heat (J/ (gm K)	0.72	0.134	0.72
Thickness (nm)	50	100	50
Sublimation or melting limit (°C)	2227	3422	2227

PROTON BEAM	RHIC 2017	EIC	XX bunch
Beam rms width (mm)	0.68	1.2	
# of protons per bunch	1.60E+11	6.90E+10	
# of bunches	111	1160	

Thermal conductivity multiplier	1
Simulation time step (ns)	500

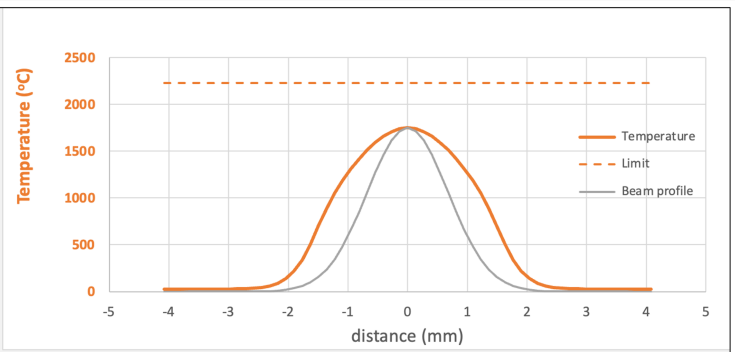

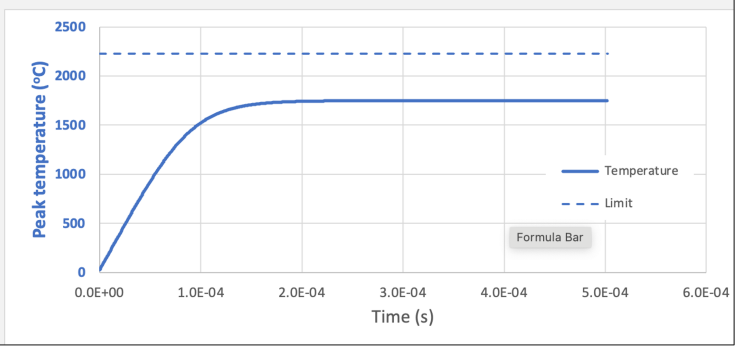

Carbon target temperatures from Thieberger's estimate

EIC for highest luminosity

- 1160 bunches
- 6.9×10^{10} protons per bunch
- $\sigma_r^{95} = 1.2\,\text{mm}$ cooled beam

TARGET	GRAPHITE	TUNGSTEN	CARBON
Density (g/cc)	2.26	19.3	2.26
LET (MeV cm^2/g)	1.76E-03	1.12E-03	6.33E-04
Thermal conductivity [W/(K * m)]	390	173	390
Emissivity	0.8	0.35	0.8
Specific heat (J/ (gm K)	0.72	0.134	0.72
Thickness (nm)	50	100	50
Sublimation or melting limit (°C)	2227	3422	2227

PROTON BEAM	RHIC 2017	EIC	XX bunch
Beam rms width (mm)	0.68	1.2	
# of protons per bunch	1.60E+11	6.90E+10	
# of bunches	111	1160	

Thermal conductivity multiplier	1
Simulation time step (ns)	500

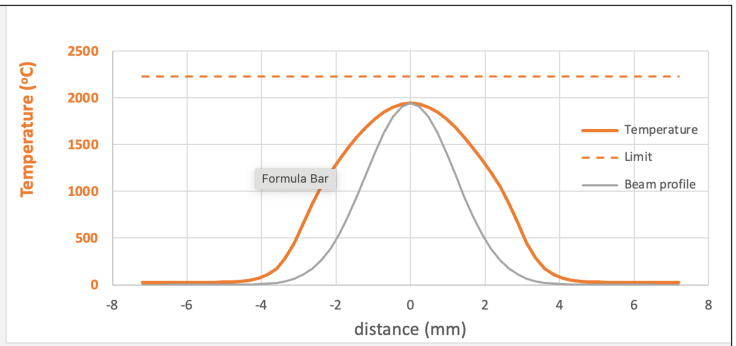

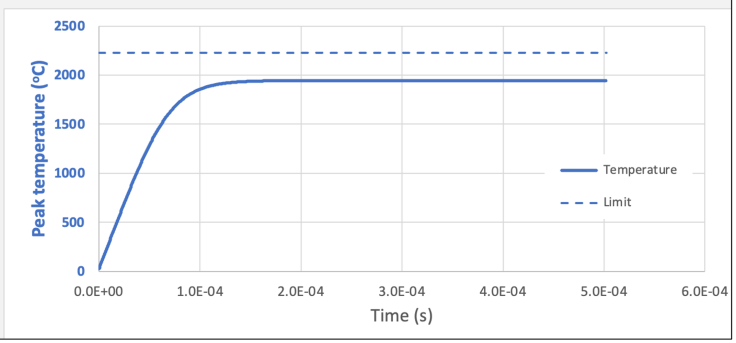

Direct measurement of target temperature

Direct determination of target temperature

- measurement of visible and infrared light
- present light-collecting lens badly aligned on C target interaction region
  - C target chamber was already pumped down when equipment became available
  - Need dedicated APEX next year to align with *open* C target chamber
  - Calibration of signal temperature using 1:1 lab setup at 2500 K oven


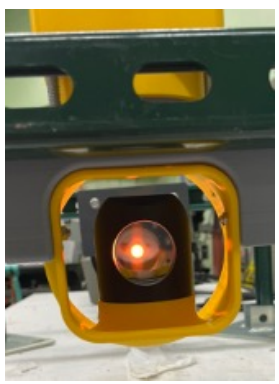


Conclusion I

1. Bunch-induced depolarization in H target
   - RHIC: harmonic numbers > 350 were ignored
   - EIC: All depolarizing transitions appear at harmonic numbers < 50
2. Beam-induced magnetic fields perturb target polarization
   - RHIC: Magnetic field involved: $B(r) \leq 2.3\,\mathrm{mT}$
   - EIC: uncooled $B(r) < 4.9\,\mathrm{mT}$
   - EIC: cooled $B(r) < 11.7\,\mathrm{mT}$
3. Holding field of $|\vec{B}| \geq 300\,\mathrm{mT}$ avoids beam-induced depolarization
   - Concept using permanent magnets (NdFeB) appears feasible
   - Allows for orientation of holding field $\vec{B}$ in any direction (along x, y, or z)
   - System will allow to provide holding field $\vec{B} = 0$
   - No zero crossings along ABS axis, $|\vec{B}(0, y, 0)| \gtrsim 1.9\,\mathrm{mT}$
   - May need compensation scheme to make $\int B_{x,y,z} \mathrm{d}\ell = 0$ along beam (z) axis
     - What's the spin rotation angle along the beam (z) axis?
     - Tolerable? Does one need compensation beyond $\int B \mathrm{d}\ell = 0$?

Conclusion II

4. C targets
   - Heating at highest EIC luminosity will be about same as at RHIC, due to much larger β function at IP4 compared to IP12
   - C target holder need to be redesigned to minimize increased RF heating at EIC
   - Direct C target temperature measurement underway to further mitigate risk
5. $^3\vec{\text{He}}$ atomic beam source under development by MIT
   - ideally suited for EIC
   - Polarimetry section in IP4 looks good
6. $\vec{\text{D}}$ and $^3\vec{\text{He}}$ atomic targets at EIC
   - Study bunch-induced depolarization
   - Study beam-induced $\vec{B}$ field effects on target polarizations

Conclusion III

Other things that need to be looked into

1. Zero-crossings along the vertical axis of present HJET
   - Revisit magnetic field calculations of HJET holding field → in progress.
   - Measure holding field in target region and estimate hysteresis effects
2. Polarization measurements using all transition units in ABS and BRP
3. Tracking of atoms in HJET & sextupole magnet systems
   - Recuperated tracking code used originally for HJET design from Michelle/Paolo → will be time consuming to make it work

Back to my initial observation I

- Need broad discussion on approaching tasks and rejuvenating polarization technology for the EIC's success.
- Key issues include funding, talent recruitment, and securing long-term commitment of new partner institutions.
- Future of spin physics with $\vec{d}$ and $^3\overrightarrow{\mathrm{He}}^{++}$ beams will no longer even be an option if we wait a few more years to get our act together.
- Large scale of young talent needed to advance polarized beams at EIC: Timescales involved are long compared to EIC's anticipated lifetime.
- Funding and support for AGS operations should be allocated for polarization technology development *outside* of the EIC project.
  - HJET/DJET system for AGS reduces unwanted polarization components to optimize polarization transmission *before* EIC commissioning.
  - Using AGS for polarization development could save months in EIC commissioning, reduce costs, and accelerate first physics with polarized beams.

Back to my initial observation II

- Organize workshops and attract groups from national and international scientific community to work on polarization technology.
  Two upcoming workshops:
  1. **Polarized Sources, Targets, and Polarimetry**
     Organizer: D. Gaskell
     Date: Sep. 22 – Sep. 27, 2024
     Location: JLAB
  2. **Polarized Ion Sources and Beams at EIC** (approved by the CFNS)
     Organizers: J. Datta, Z.-E. Meziani, R. Milner, D. Raparia, FR
     Date: week of March 3 – 5, 2025
     Location: Stony Brook

References I

[1] W. Haeberli, "H-jet measures beam polarization at RHIC," CERN Cour. **45N8**, 15 (2005).

[2] N. Akchurin, J. Langland, Y. Onel, B. E. Bonner, M. D. Corcoran, J. Cranshaw, F. Nessi-Tedaldi, M. Nessi, C. Nguyen, J. B. Roberts, et al., "Analyzing power measurement of pp elastic scattering in the coulomb-nuclear interference region with the 200-gev/c polarized-proton beam at fermilab," Phys. Rev. D **48**, 3026 (1993), URL https://link.aps.org/doi/10.1103/PhysRevD.48.3026.

[3] I. G. Alekseev, A. Bravar, G. Bunce, S. Dhawan, K. O. Eyser, R. Gill, W. Haeberli, H. Huang, O. Jinnouchi, A. Kponou, et al., "Measurements of single and double spin asymmetry in *pp* elastic scattering in the cni region with a polarized atomic hydrogen gas jet target," Phys. Rev. D **79**, 094014 (2009), URL https://link.aps.org/doi/10.1103/PhysRevD.79.094014.

[4] N. H. Buttimore, "A Helium-3 polarimeter using electromagnetic interference," PoS **PSTP2013**, 057 (2013).

[5] M. Diermaier, C. B. Jepsen, B. Kolbinger, C. Malbrunot, O. Massiczek, C. Sauerzopf, M. C. Simon, J. Zmeskal, and E. Widmann, "In-beam measurement of the hydrogen hyperfine splitting and prospects for antihydrogen spectroscopy," Nature Commun. **8**, 5749 (2017), 1610.06392.

[6] A. Airapetian, N. Akopov, Z. Akopov, M. Amarian, A. Andrus, E. Aschenauer, W. Augustyniak, R. Avakian, A. Avetissian, E. Avetissian, et al., "The hermes polarized hydrogen and deuterium gas target in the hera electron storage ring," Nuclear Instruments and Methods in Physics Research Section A: Accelerators, Spectrometers, Detectors and Associated Equipment **540**, 68 (2005), ISSN 0168-9002, URL https://www.sciencedirect.com/science/article/pii/S0168900204024167.

[7] N. Ramsey, *Molecular Beams* (Oxford University Press, 1956).

[8] S. Lee, *Accelerator Physics* (World Scientific Publishing Company, 2011), ISBN 9789814405287.

[9] F. Willeke and J. Beebe-Wang, "Electron ion collider conceptual design report 2021," (????), URL https://www.osti.gov/biblio/1765663.

References II

[10] F. Rathmann et al., "Complete angular distribution measurements of pp spin correlation parameters Axx, Ayy, and Axz and analyzing power Ay at 197.4 MeV," Phys. Rev. C **58**, 658 (1998).

[11] B. von Przewoski et al., "Proton proton analyzing power and spin correlation measurements between 250-MeV and 450-MeV at $7^\circ \leq \theta(c.m.) \leq 90^\circ$ with an internal target in a storage ring," Phys. Rev. C **58**, 1897 (1998).

[12] B. von Przewoski, H. O. Meyer, P. V. Pancella, S. F. Pate, R. E. Pollock, T. Rinckel, F. Sperisen, J. Sowinski, W. Haeberli, W. K. Pitts, et al., "Absolute measurement of the p+p analyzing power at 183 mev," Phys. Rev. C **44**, 44 (1991), URL https://link.aps.org/doi/10.1103/PhysRevC.44.44.

[13] G. Plattner and A. Bacher, "Absolute calibration of spin-$\frac{1}{2}$ polarization," Physics Letters B **36**, 211 (1971), ISSN 0370-2693, URL https://www.sciencedirect.com/science/article/pii/0370269371900712.

[14] P. Blümler and H. Soltner, "Practical Concepts for Design, Construction and Application of Halbach Magnets in Magnetic Resonance," Applied Magnetic Resonance **54**, 1701 (2023), ISSN 1613-7507, URL https://doi.org/10.1007/s00723-023-01602-2.

[15] H. Soltner and P. Blümler, "Dipolar halbach magnet stacks made from identically shaped permanent magnets for magnetic resonance," Concepts in Magnetic Resonance Part A **36A**, 211 (2010), https://onlinelibrary.wiley.com/doi/pdf/10.1002/cmr.a.20165, URL https://onlinelibrary.wiley.com/doi/abs/10.1002/cmr.a.20165.

[16] H. Raich and P. Blümler, "Design and construction of a dipolar halbach array with a homogeneous field from identical bar magnets: Nmr mandhalas," Concepts in Magnetic Resonance Part B: Magnetic Resonance Engineering **23B**, 16 (2004), https://onlinelibrary.wiley.com/doi/pdf/10.1002/cmr.b.20018, URL https://onlinelibrary.wiley.com/doi/abs/10.1002/cmr.b.20018.

References III

[17] B. v. Przewoski et al., "Analyzing powers and spin correlation coefficients for $p + d$ elastic scattering at 135 and 200 MeV," Phys. Rev. C **74**, 064003 (2006), URL http://link.aps.org/doi/10.1103/PhysRevC.74.064003.

[18] R. E. Pollock, W. A. Dezarn, M. Dzemidzic, J. Doskow, J. G. Hardie, H. O. Meyer, B. v. Przewoski, T. Rinckel, F. Sperisen, W. Haeberli, et al., "Calibration of the polarization of a beam of arbitrary energy in a storage ring," Phys. Rev. E **55**, 7606 (1997), URL https://link.aps.org/doi/10.1103/PhysRevE.55.7606.

Spare slides

Critical field for hydrogen hyperfine splitting I

Zeeman region:

- magnetic flux density at which energy separation between different hyperfine levels becomes comparable to Zeeman splitting.
- referred to as *critical magnetic field* or *Breit-Rabi field* B_c
- Breit-Rabi formula (energy levels of hydrogen atom in external magnetic field:

$$E_{F,m_F} = -\frac{E_{\mathrm{hfs}}}{2(2I+1)} + g_J \mu_B m_J B \pm \frac{E_{\mathrm{hfs}}}{2}\sqrt{1+\frac{2m_F x}{F}+x^2}\,, \text{where} \qquad (27)$$

- E_{hfs} is hyperfine splitting energy
- I is nuclear spin (for H, $I = \frac{1}{2}$)
- g_J is Landé g-factor
- μ_B is Bohr magneton
- m_J is magnetic quantum number
- m_F is total angular momentum quantum number
- $x = \frac{g_J \mu_B B}{E_{\mathrm{hfs}}}$
- $F = I + J$ is total angular momentum (for H, $J = \frac{1}{2}$)

Critical field for hydrogen hyperfine splitting II

For H:

- hyperfine splitting energy E_{hfs} (1420 MHz):

$$E_{\mathrm{hfs}} \approx 5.874 \times 10^{-6}\,\mathrm{eV} \tag{28}$$

- Critical field B_c is when Zeeman energy $g_J \mu_B B$ is comparable to E_{hfs}. With $g_J \mu_B B_c \approx E_{\mathrm{hfs}}$, we get:

$$B_c \approx \frac{E_{\mathrm{hfs}}}{g_J \mu_B} \tag{29}$$

- For H, $g_J \approx 2$ (approximately for electron), and $\mu_B \approx 5.788 \times 10^{-5}\,\mathrm{eV/T}$. Thus,

$$B_c \approx \frac{5.874 \times 10^{-6}\,\mathrm{eV}}{2 \times 5.788 \times 10^{-5}\,\mathrm{eV/T}} \approx 50.7\,\mathrm{mT} \tag{30}$$

Detector symmetry required to accomplish the task

For spin $\frac{1}{2}$ + spin $\frac{1}{2}$ scattering, suitable geometry below shows pattern of detected azimuthal angles [10].

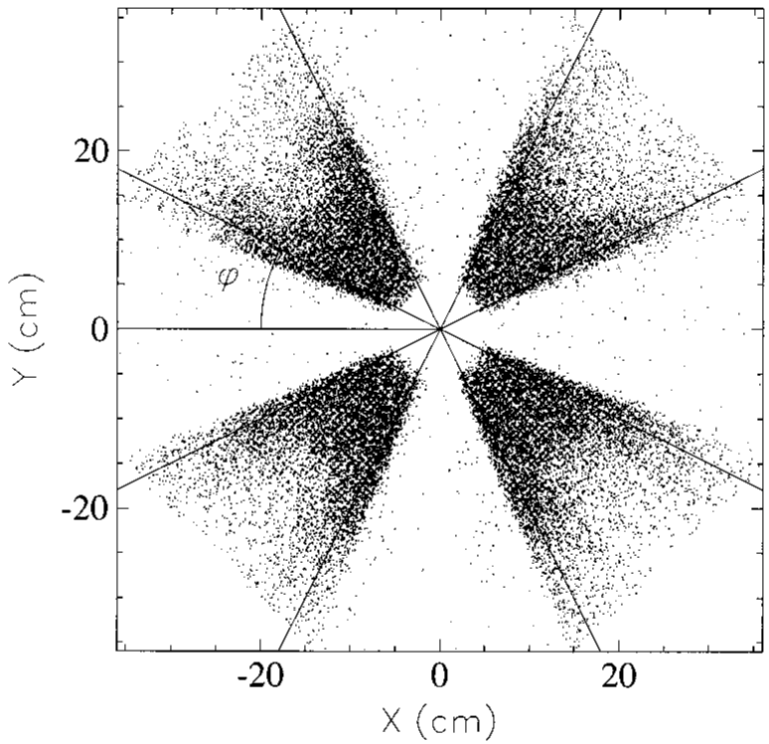

For spin $\frac{1}{2}$ + spin 1 scattering, a higher segmentation is needed, because besides $\sin\phi$ and $\sin 2\phi$, also terms $\sin 3\phi, \ldots$ contribute to asymmetries [17].

Polarization of beam $\vec{P}$ and target $\vec{Q}$ [10, 11]

	$\pm x$		$\pm y$		$\pm z$	
	PRE	POST	PRE	POST	PRE	POST
P_x	0.0052(47)	0.0089(44)	0.0052(47)	0.0089(44)	0.0052(47)	0.0089(44)
P_y [a]	**0.5801(34)**	**0.5425(32)**	**0.5802(34)**	**0.5417(32)**	**0.5765(34)**	**0.5447(32)**
P_z	−0.0021(47)	0.0003(44)	−0.0021(47)	0.0003(44)	−0.0021(47)	0.0003(44)
Q_x	**0.7401(59)**	**0.7394(56)**	−0.0039(59)	0.0039(56)	−0.0071(23)	−0.0052(23)
Q_y	0.0111(59)	0.0039(56)	**0.7400(59)**	**0.7406(56)**	−0.0055(59)	−0.0034(56)
Q_z	0.0158(60)	0.0240(60)	−0.0174(61)	−0.0121(61)	**0.7401(42)** [b]	**0.7400(40)** [b]
S_{P_y}	−0.0008(18)	−0.0005(17)	−0.0008(18)	0.0005(17)	−0.0008(18)	0.0005(17)
S_{Q_x}	0.0017(23)	−0.0007(23)	−0.0040(23)	−0.0031(23)	−0.0043(23)	−0.0024(23)
S_{Q_z}	−0.0091(82)	−0.0162(82)	−0.0177(82)	−0.0197(82)	0.0013(82)	−0.0086(82)

- Beam polarization export/calibration to arbitrary energy [18]
  - PRE ≡ b (197.4 MeV)
  - Export ≡ c (399.1 MeV)
  - POST ≡ d (197.4 MeV)